Development of superconducting multiqubit devices

I.N. Moskalenko, V. V. Ryazanov, I.S. Besedin, N.N. Abramov and A.V. Ustinov

Contents

- Introduction
- Transmon qubit
- Readout
- Chain of 11 qubits
- Array of 25 qubits
- Fluxonium qubit
- Conclusion

Quantum processors – transmon based

Google
Sycamore processor

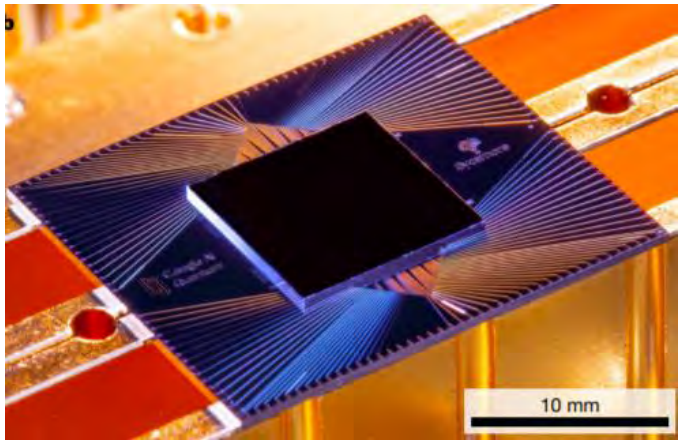

*Arute, F., *et al.* *Nature* **574,** 505–510 (2019)

IBM Quantum
27-qubit Falcon

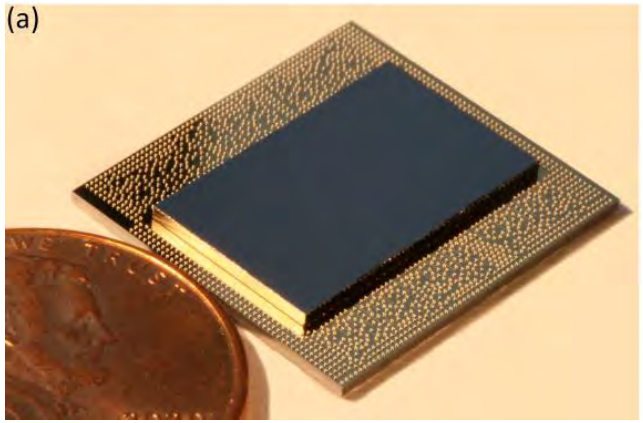

*Petar Jurcevic, et al. arXiv:2008.08571, 19 Aug 2020

56-qubit *Zuchongzhi*

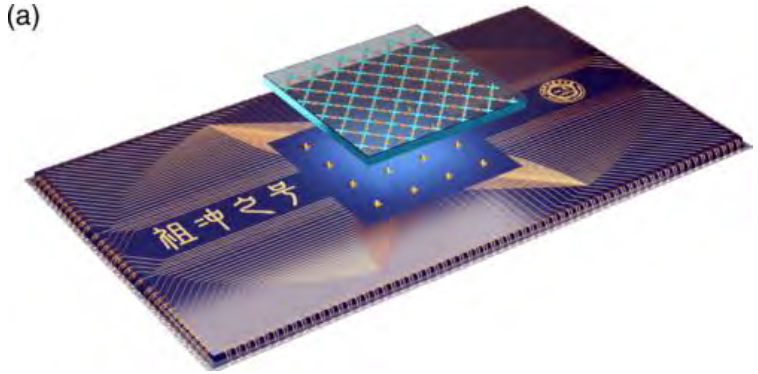

*Yulin Wu *et al.* Phys. Rev. Lett. **127**, 180501

Rigetti Computing

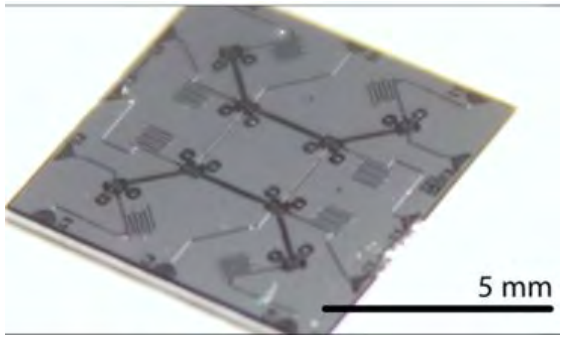

*Sabrina S. Hong, et al. Phys. Rev. A 101, 012302 (2020)

16 qubit IBM

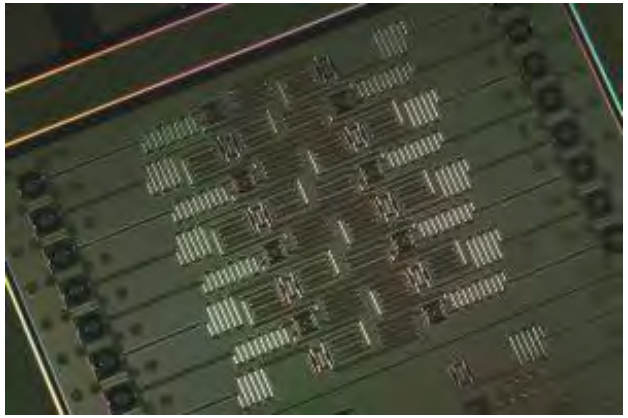

*Wang, Y., *et al. npj Quantum Inf* **4,** 46 (2018)

127-qubit Eagle processor

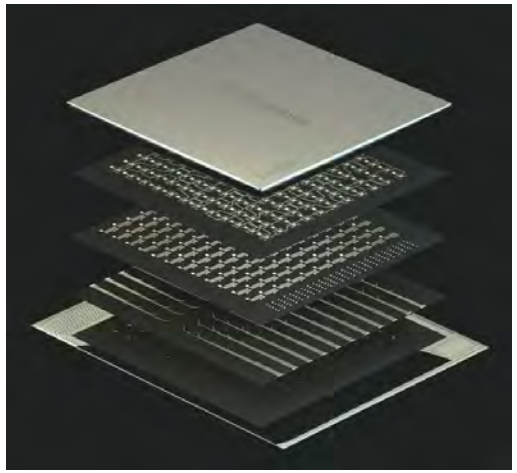

*https://newsroom.ibm.com/2021-11-16-IBM-Unveils-Breakthrough-127-Qubit-Quantum-Processor

Superconducting charge qubit (Cooper-pair box)

Charge Qubit

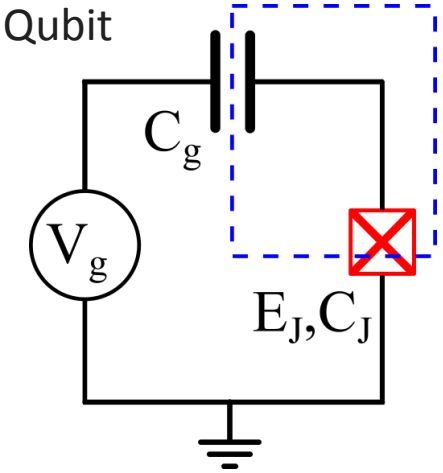

Circuit QED*

$$\hat{n} = -i\frac{\partial}{\partial\phi}$$

$$[\hat{\phi}, \hat{n}] = i\hbar$$

Hamiltonian:

$$H_{CPB} = 4E_C(n - n_g)^2 + E_J(1 - \cos\phi)^{**},$$

$$E_C = \frac{4e^2}{2(C_g + C_J)}, \qquad E_C \gg E_J$$

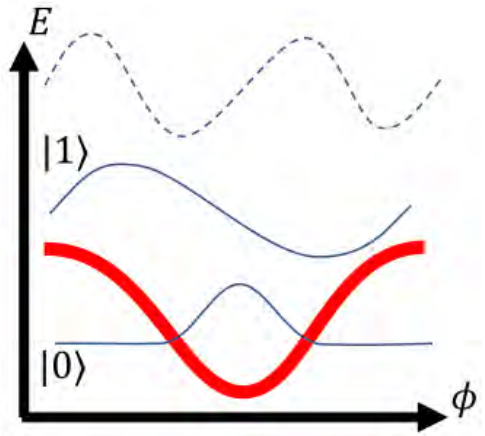

$T_{1,2} \sim 200 \div 300\ ns$

Transmon Qubit *

*Uri Vool, Michel H. Devoret, arXiv:1610.03438

** Jens Koch, et al., Phys. Rev. A, B76 (4), 042319 (2007)

Transmon qubit

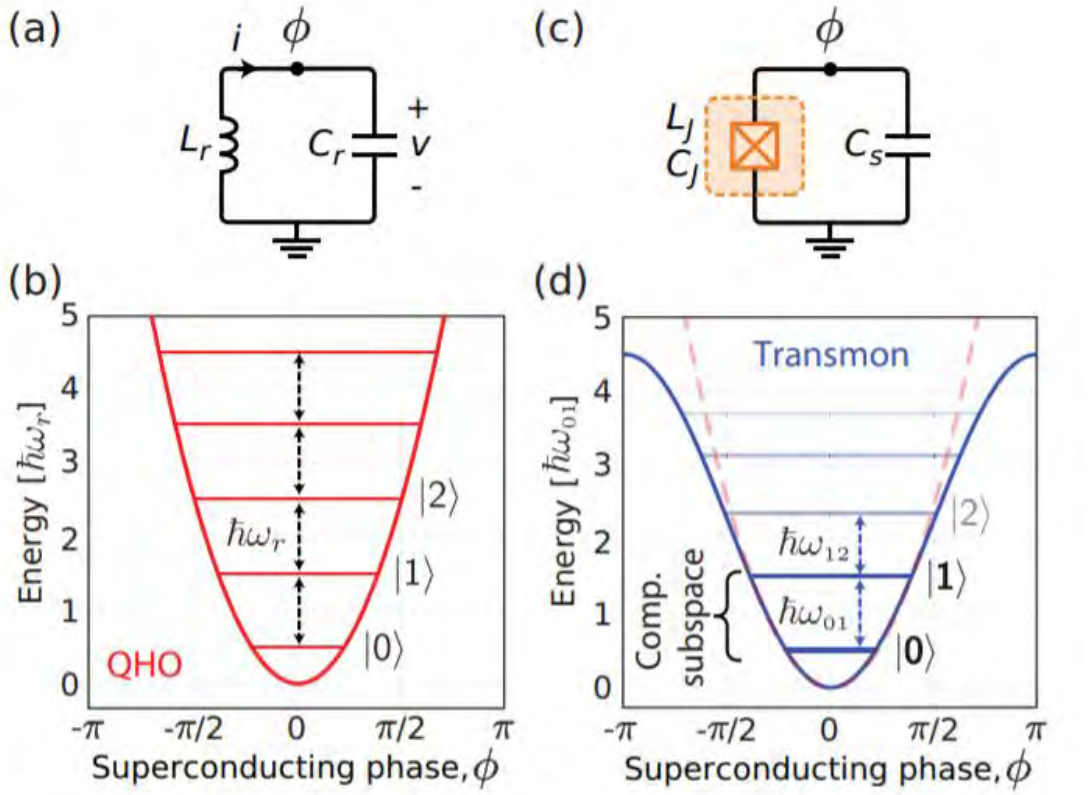

$$H_{tr} = 4E_C(n-n_g)^2 + E_J(1-\cos\phi)^*,$$

$$\left(E_C \ll E_J\right),$$

$$H_{tr} \approx 4E_C(N)^2 + \frac{E_J}{2}\phi^2 - \frac{E_J}{24}\phi^4$$

$$\alpha = \hbar\omega_{12} - \hbar\omega_{01} \sim -E_C \quad - \text{ anharmonicity}$$

Dielectric losses ➡ $T_1 = 100 \div 150\mu s^{**}$ since 2012** and up to date***

Charge dispersion**

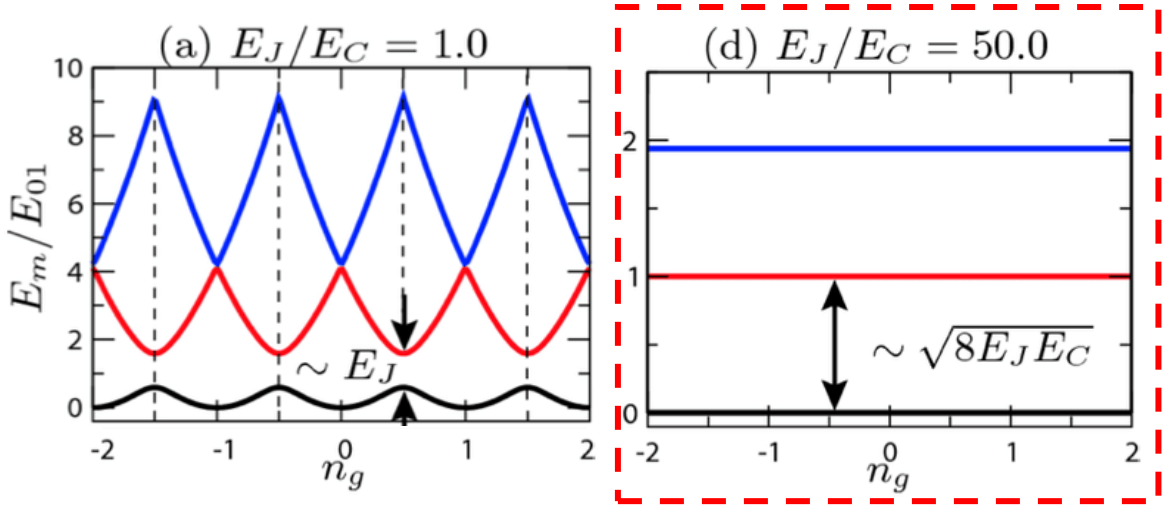

*Jens Koch, et al., Phys. Rev. A, B. 76 (4), 042319 (2007)
**M. H. Devoret, R. J. Schoelkopf, Science 339, 1169 (2013)
***A. Nersisyan, et al., arXiv preprint arXiv:1901.08042 (2019)

Dispersive readout

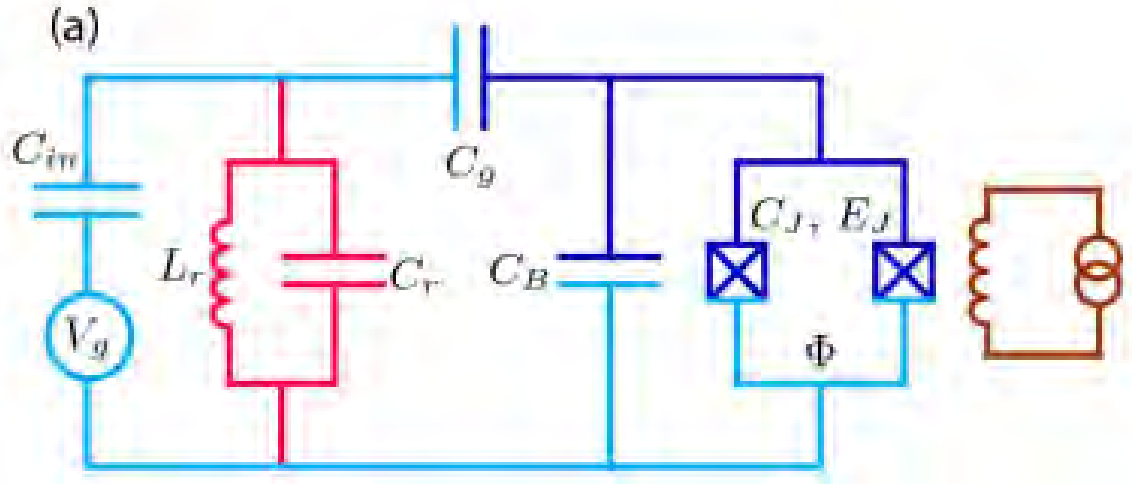

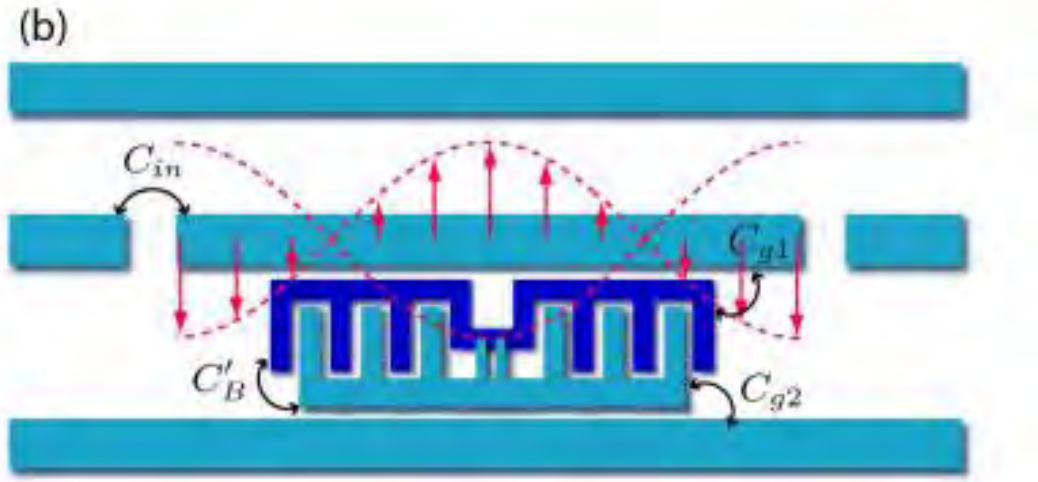

Transmon

Resonator

Interaction

$$\frac{\hat{H}}{h} = \left(f_q + \frac{\delta_q}{2}\left(\hat{a}^\dagger\hat{a} - 1\right)\right)\hat{a}^\dagger\hat{a} + f_r\hat{b}^\dagger\hat{b} + g_q\left(\hat{a}^\dagger + \hat{a}\right)\left(\hat{b}^\dagger + \hat{b}\right)$$

$$\chi_q = \frac{2g^2\delta_q}{\left(f_r - f_q\right)^2}.$$

*Jens Koch, et al., Phys. Rev. A, B. 76 (4), 042319 (2007)

Chain of 11 qubits

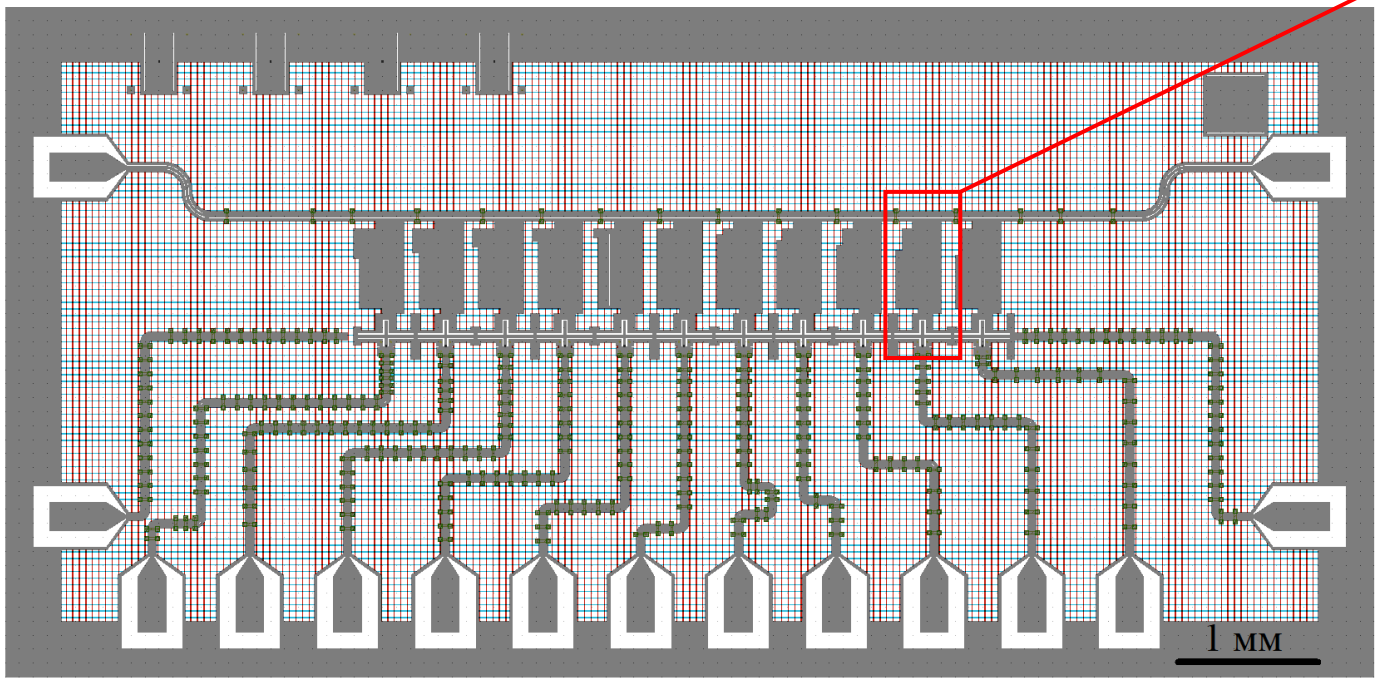

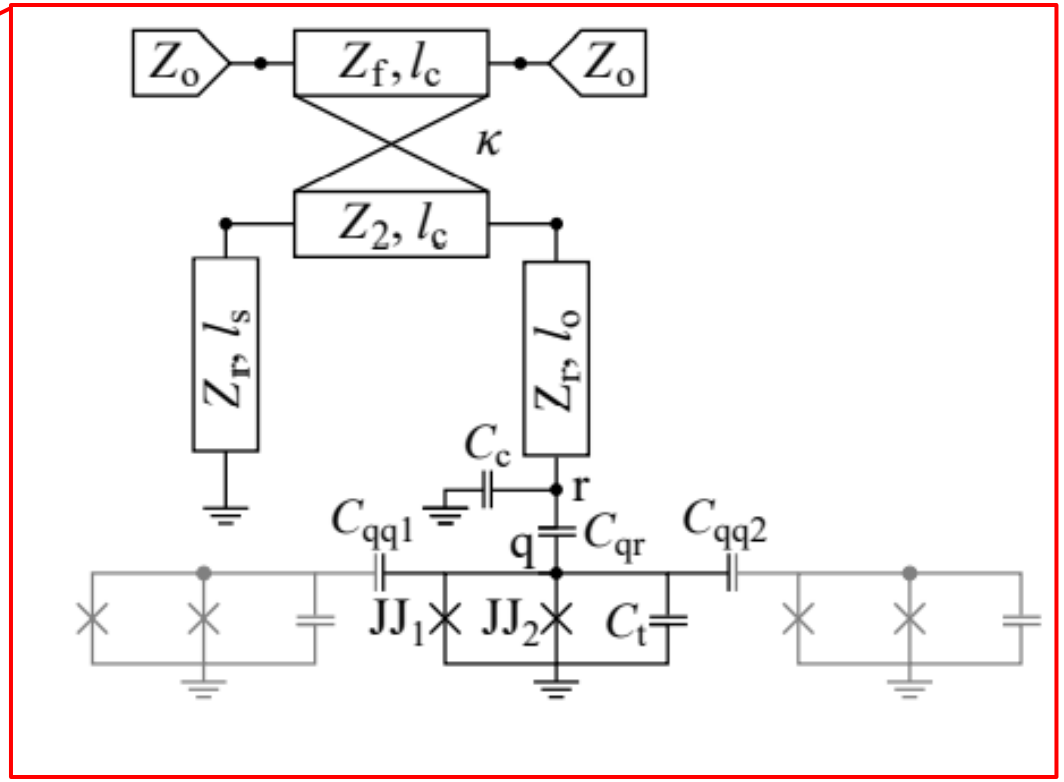

Bose-Hubbard Hamiltonian

$$\frac{H_{BH}}{h} = \sum_{q=1}^{N} \left(f_q \hat{n}_q + \frac{\delta_q}{2} \hat{n}_q \left(\hat{n}_q - 1\right)\right) + \sum_{q=1}^{(N-1)/2} \left[J_1 \hat{a}_{2q} a_{2q-1}^{\dagger} + J_2 \hat{a}_{2q} \hat{a}_{2q+1}^{\dagger} + c.c.\right]$$

- DOI: 10.1103/PhysRevB.103.224520
- Devices were fabricated at the BMSTU Nanofabrication Facility (Functional Micro/Nanosystems)

Chain of 11 qubits – Sample

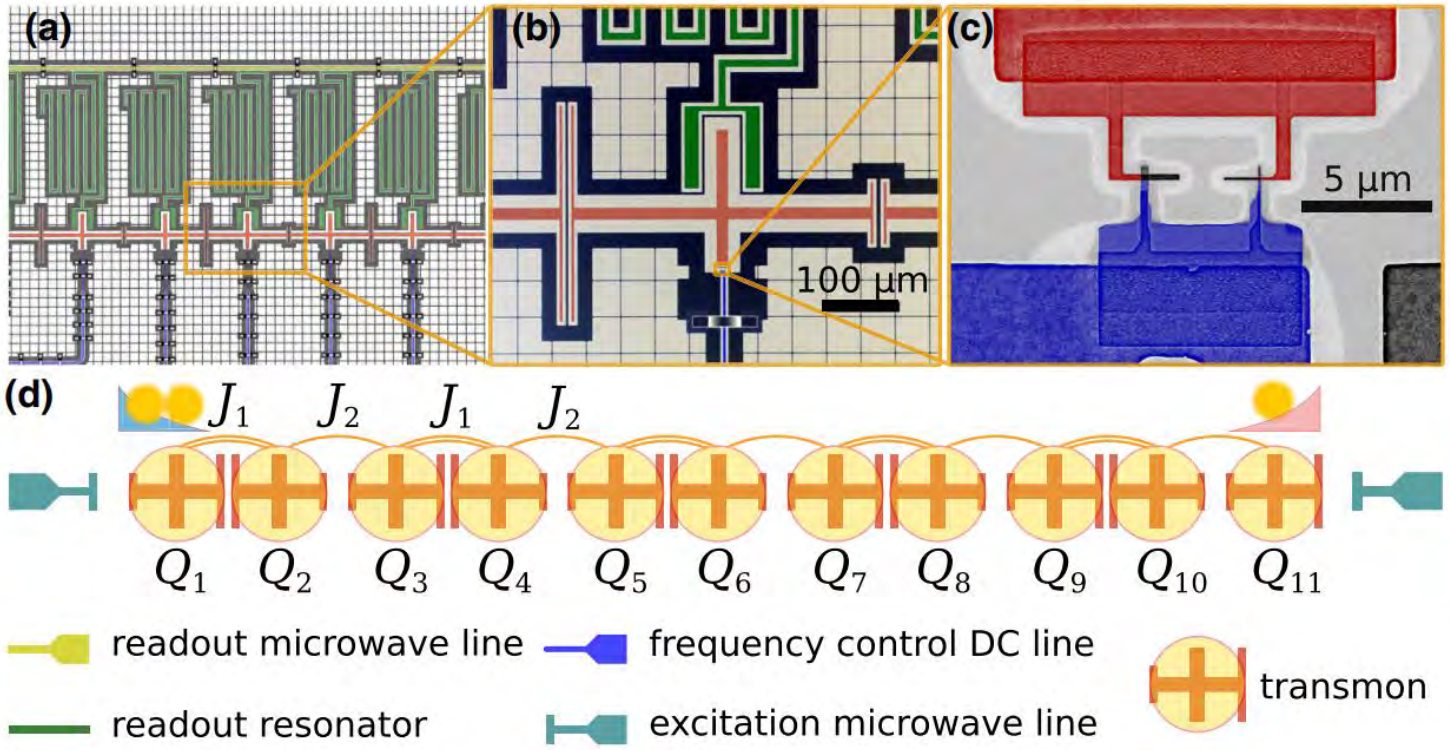

$\hat{n}_q = \hat{a}_q^\dagger \hat{a}_q$ is the photon number operator;

f_q is the eigenfrequency of q-th transmon (tuned in the range from 3.73 to 3.82 GHz);

δ_q = −155 MHz is the qubit anharmonicity;

$J_1 = 55{,}1\,\text{MHz}$ and $J_2 = 17{,}1\ \text{MHz}$ describe the nearest-neighbor coupling of qubits.

Bose-Hubbard Hamiltonian

$$\frac{H_{BH}}{h} = \sum_{q=1}^{N} \left(f_q \hat{n}_q + \frac{\delta_q}{2} \hat{n}_q \left(\hat{n}_q - 1\right)\right) + \sum_{q=1}^{(N-1)/2} \left[J_1 \hat{a}_{2q} a_{2q-1}^\dagger + J_2 \hat{a}_{2q} \hat{a}_{2q+1}^\dagger + c.c.\right]$$

- DOI: 10.1103/PhysRevB.103.224520
- Devices were fabricated at the BMSTU Nanofabrication Facility (Functional Micro/Nanosystems)

Chain of 11 qubits – Sample holder

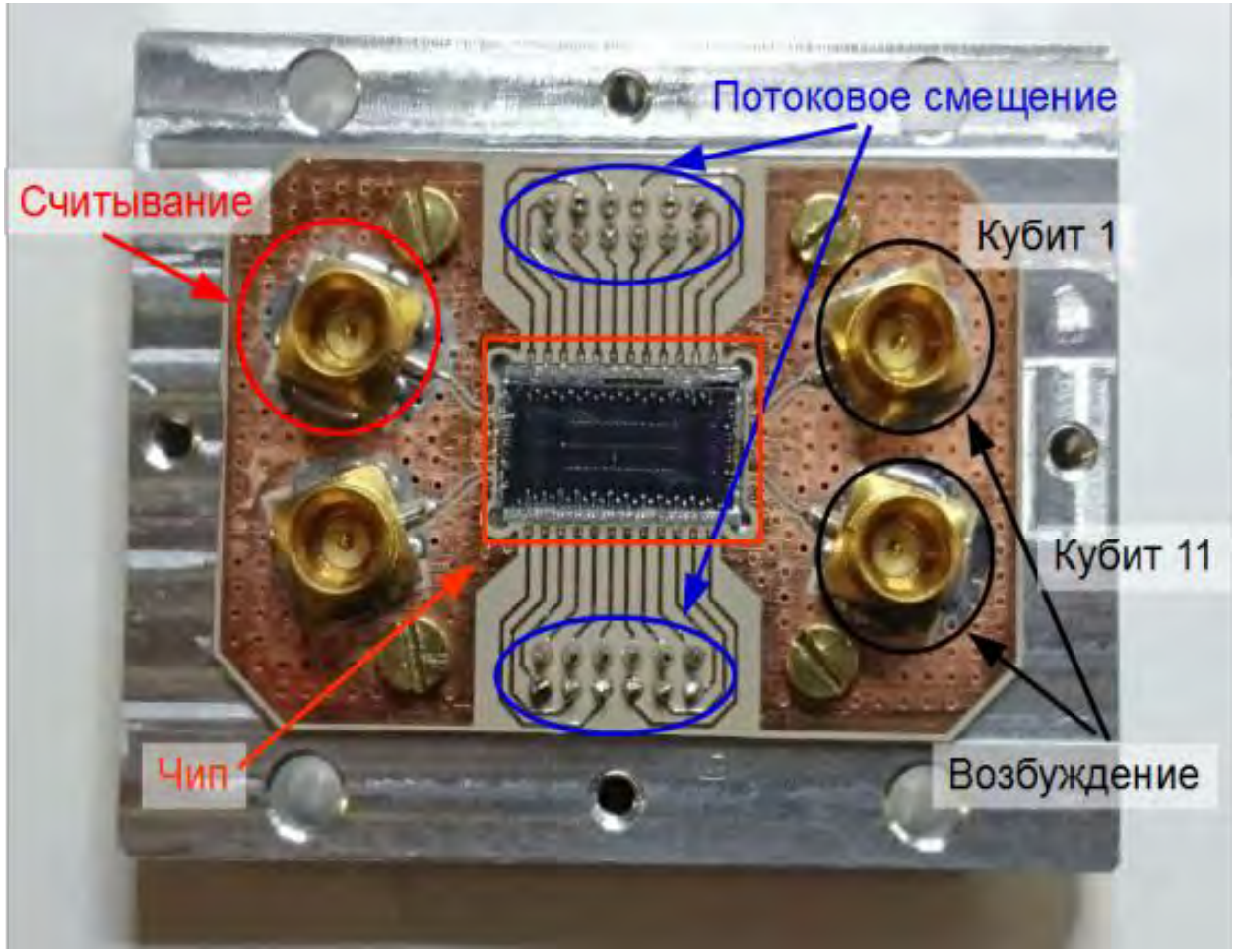

Chain of 11 qubits – Set up

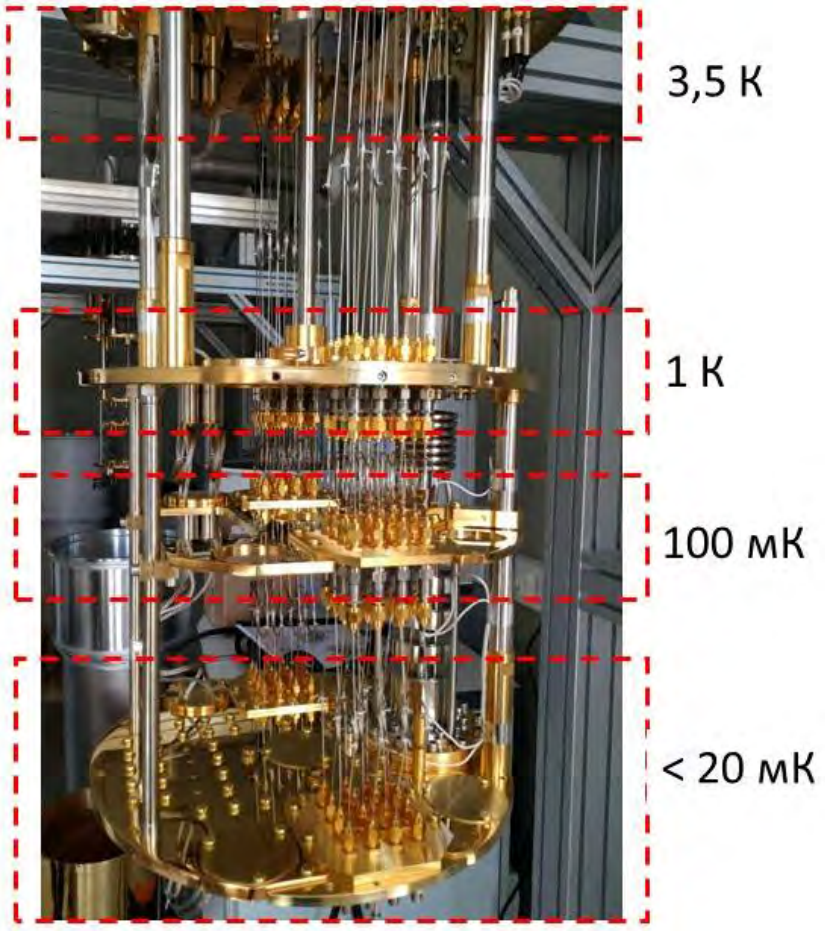

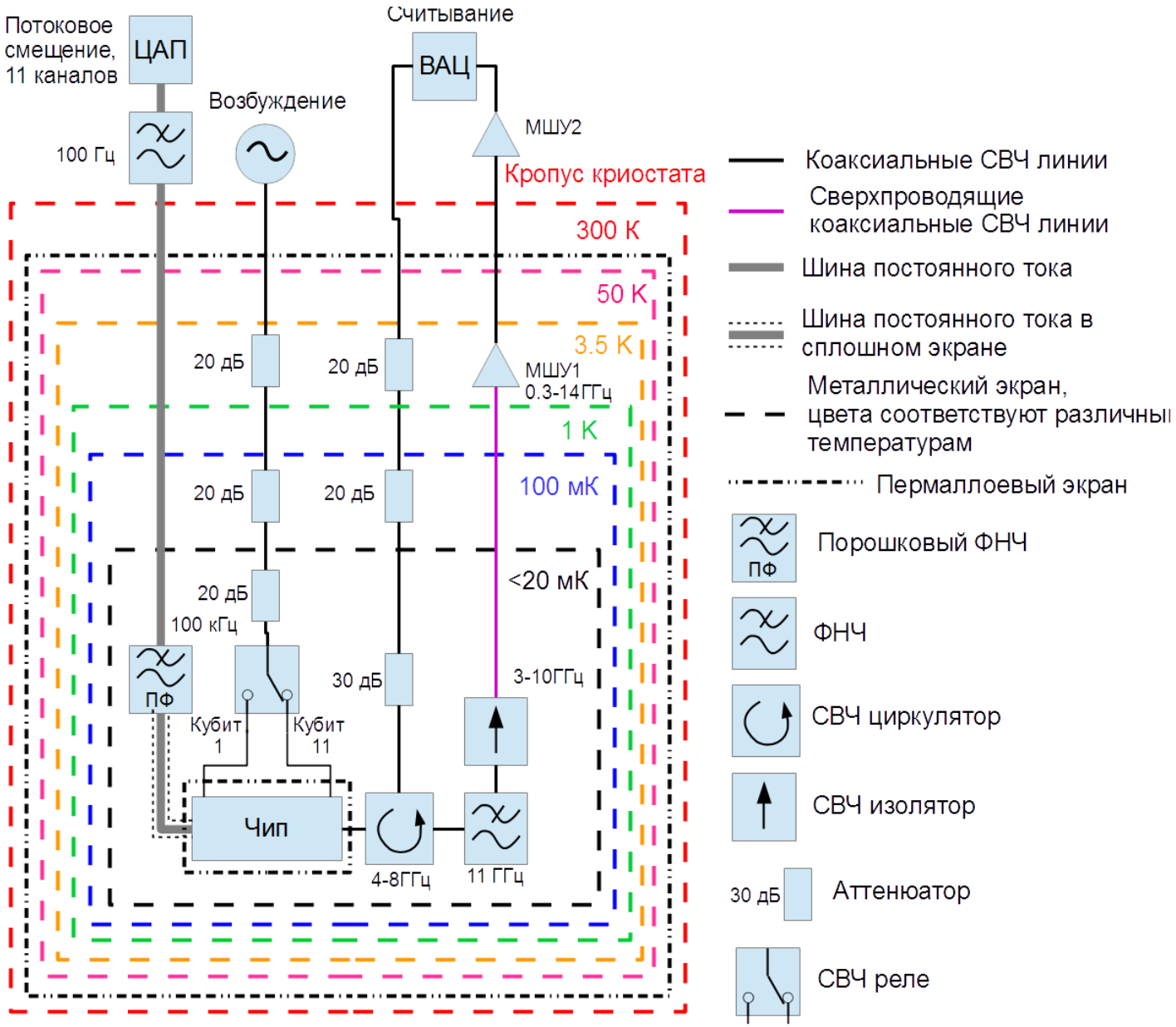

Chain of 11 qubits – Calibrations

$$f_q(\Phi_q) = \sqrt{8E_C\sqrt{\left(E_{qJ1}+E_{qJ2}\right)^2 cos^2\varphi_q + \left(E_{qJ1}-E_{qJ2}\right)^2 sin^2\varphi_q} - E_C}$$

$$\varphi_q = 2\pi\Phi_q/\Phi_0$$

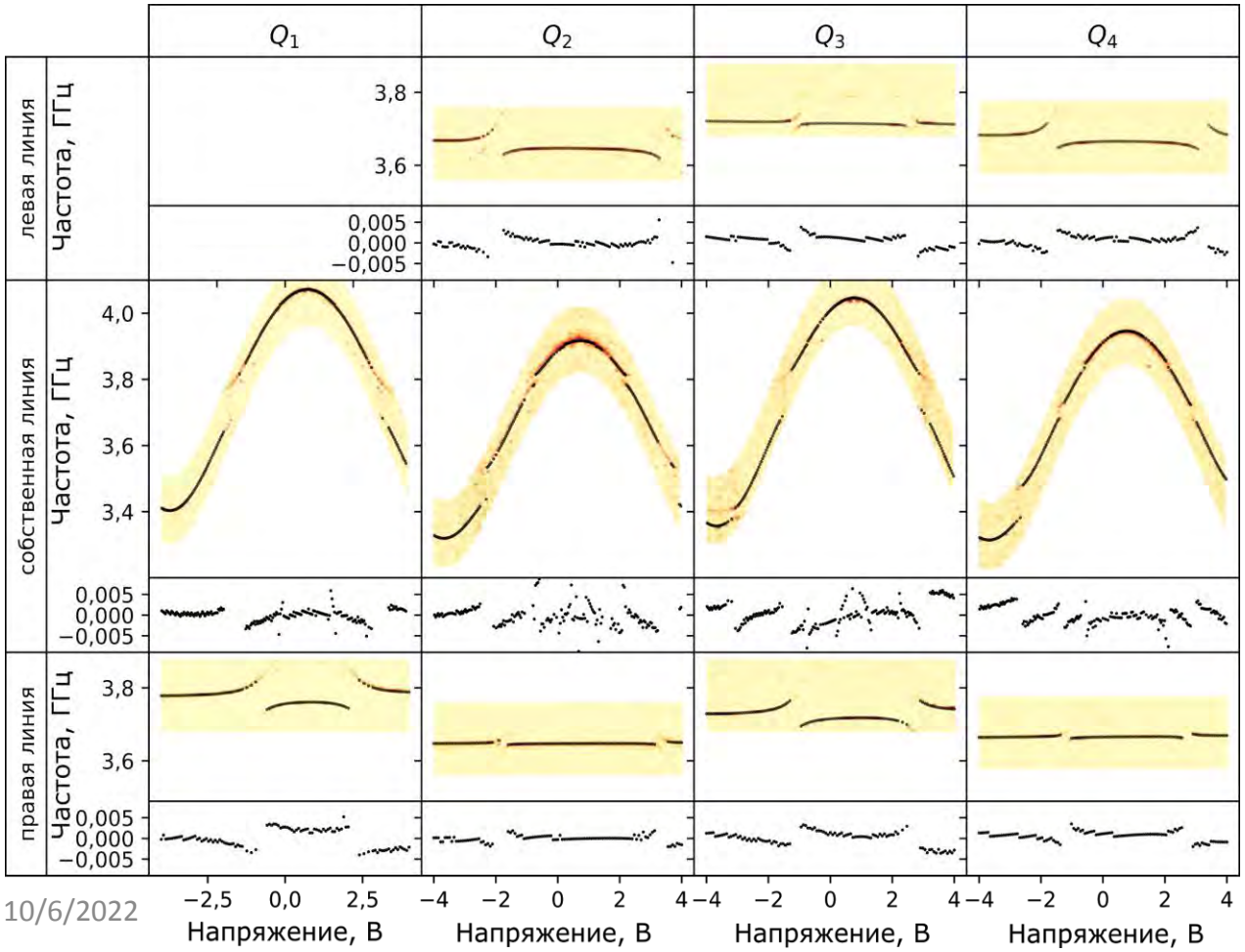

$$\Phi_q = \sum_l L_{ql} V_l + \Phi_q^0$$

$$\hat{L} = \begin{pmatrix} L_{11} & L_{12} & 0 & \cdots & 0 \\ L_{21} & L_{22} & L_{23} & \cdots & 0 \\ 0 & L_{23} & L_{33} & \cdots & 0 \\ \vdots & \vdots & \vdots & \ddots & \vdots \\ 0 & 0 & 0 & \cdots & L_{11,11} \end{pmatrix}$$

Chain of 11 qubits – Results

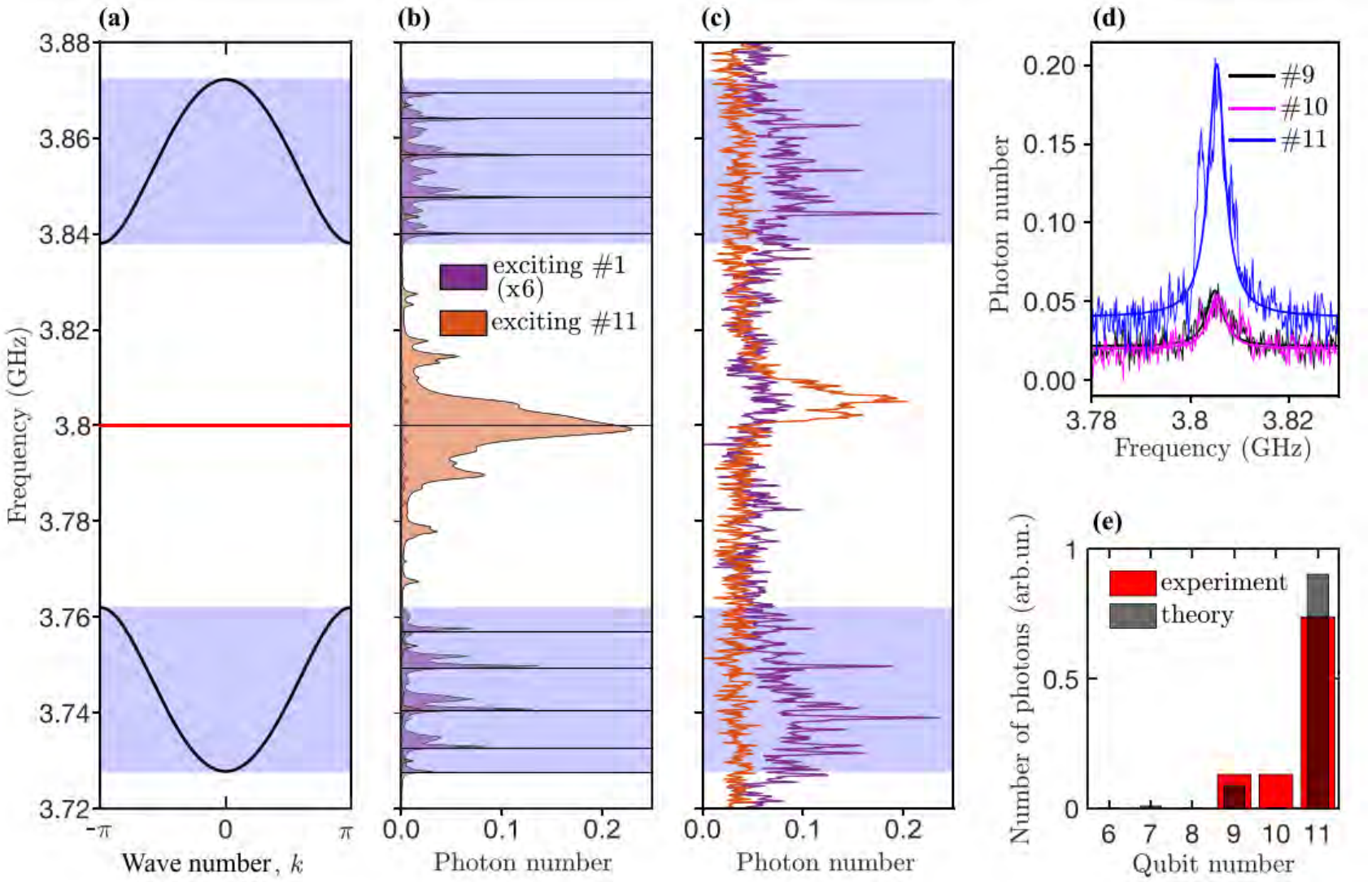

$f_0 = 3{,}8$ ГГц

Su–Schrieffer–Heeger (SSH) model

$$f = f_0 \pm \sqrt{J_1^{\,2} + J_2^{\,2} + 2J_1J_2\cos k}$$

Chain of 11 qubits – Results

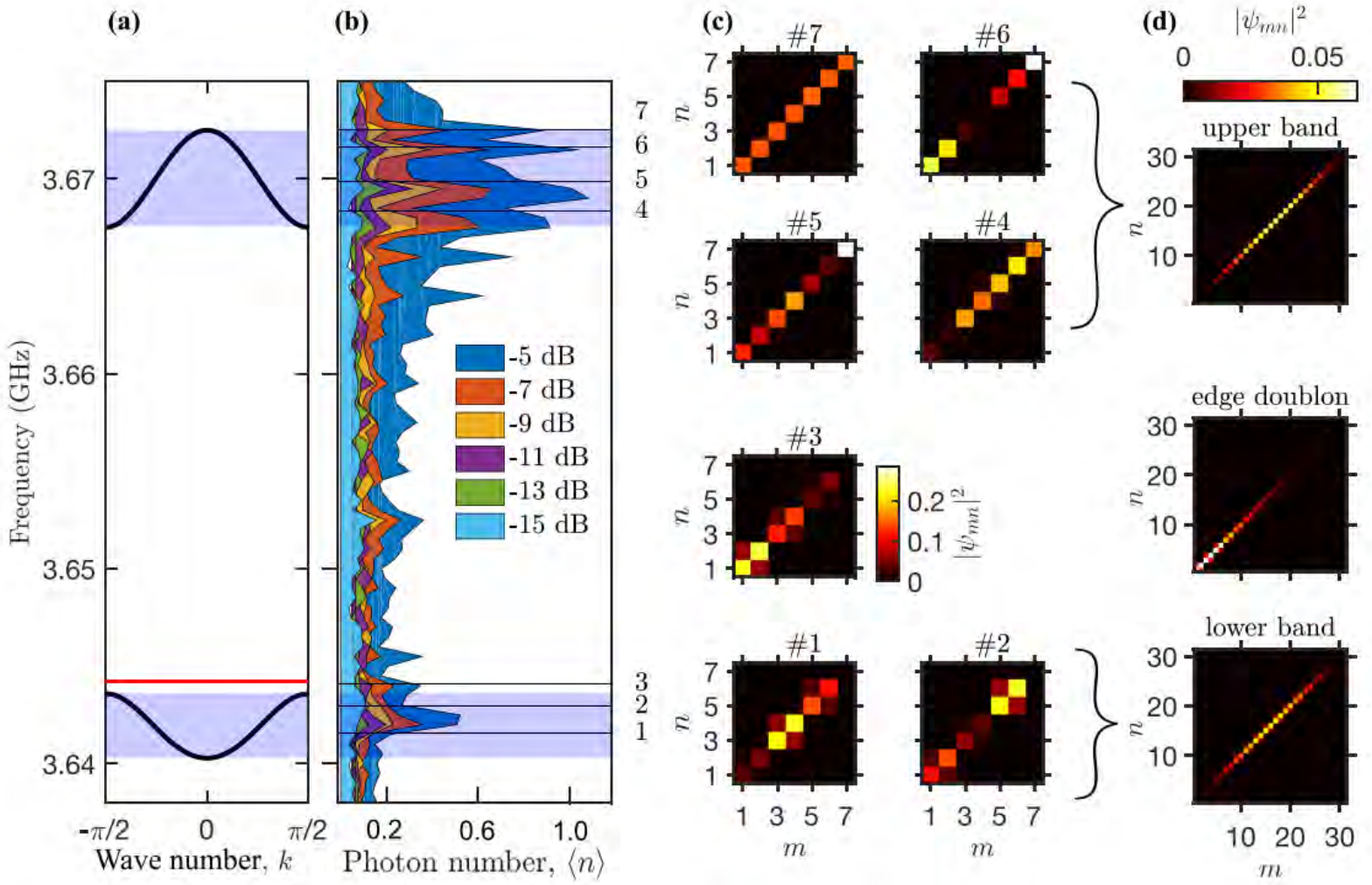

$f_0{}' = 3{,}75$ ГГц

Array of 25 qubits

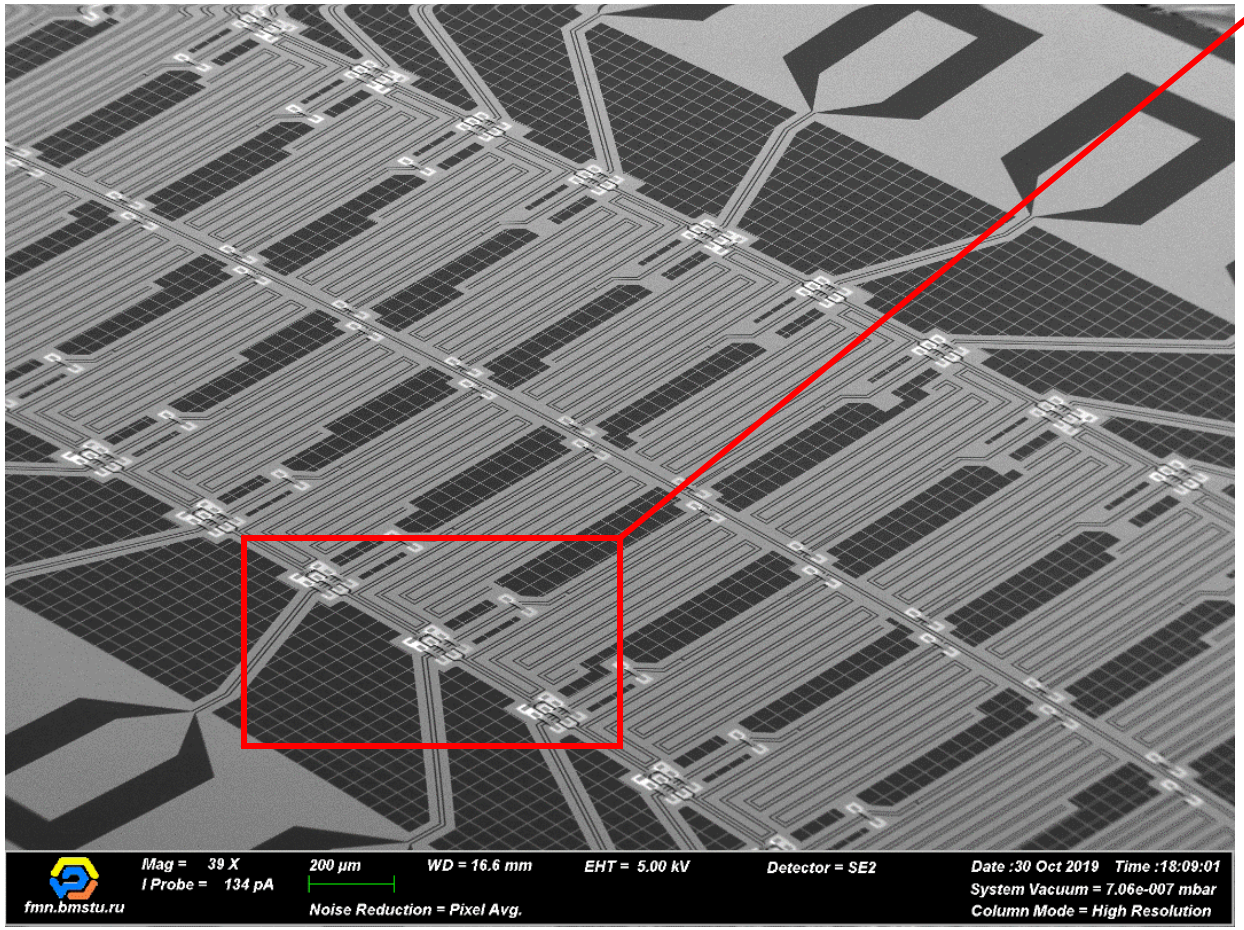

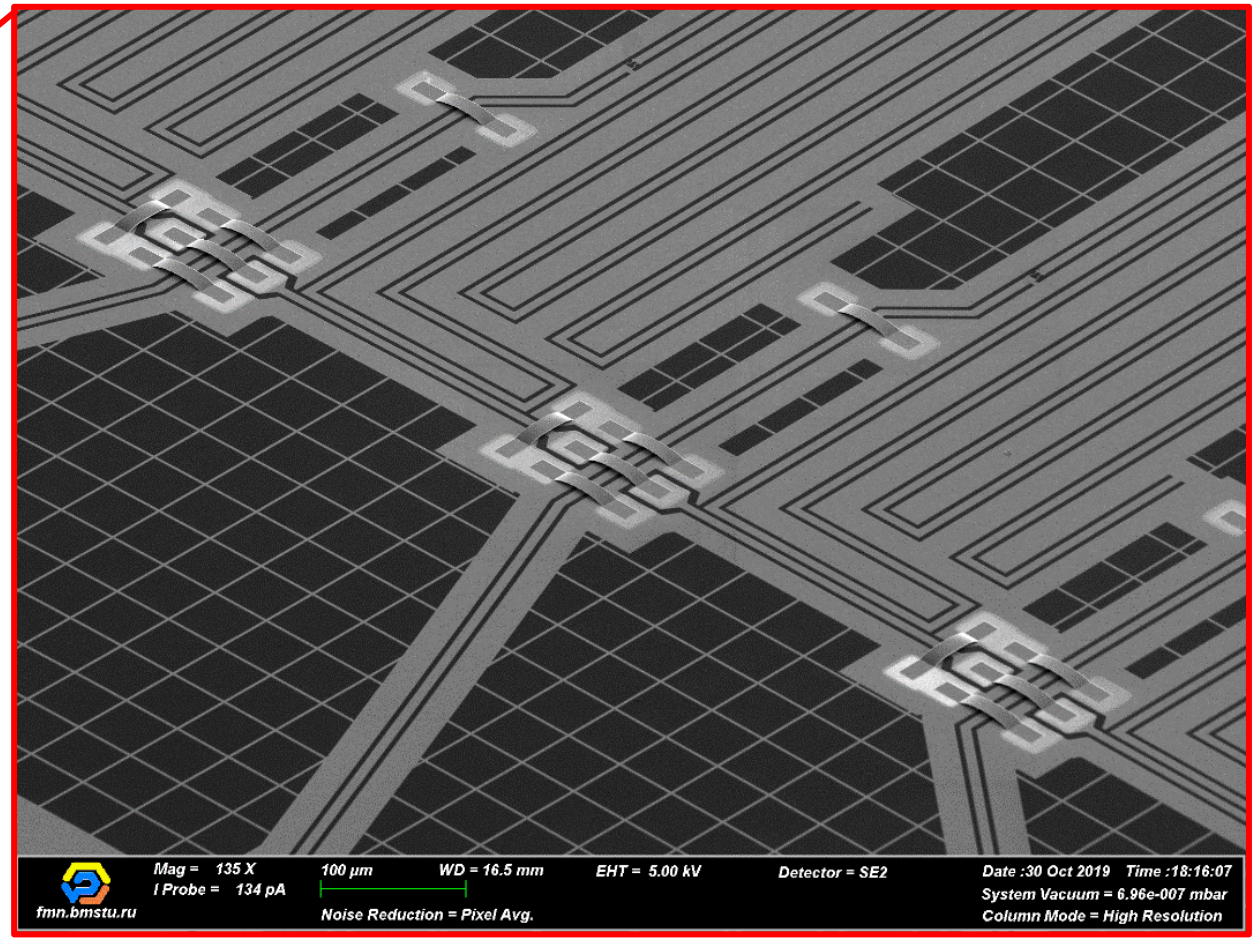

- DOI: 10.1103/PhysRevA.105.033519
- Devices were fabricated at the BMSTU Nanofabrication Facility (Functional Micro/Nanosystems)

Array of 25 qubits - Sample

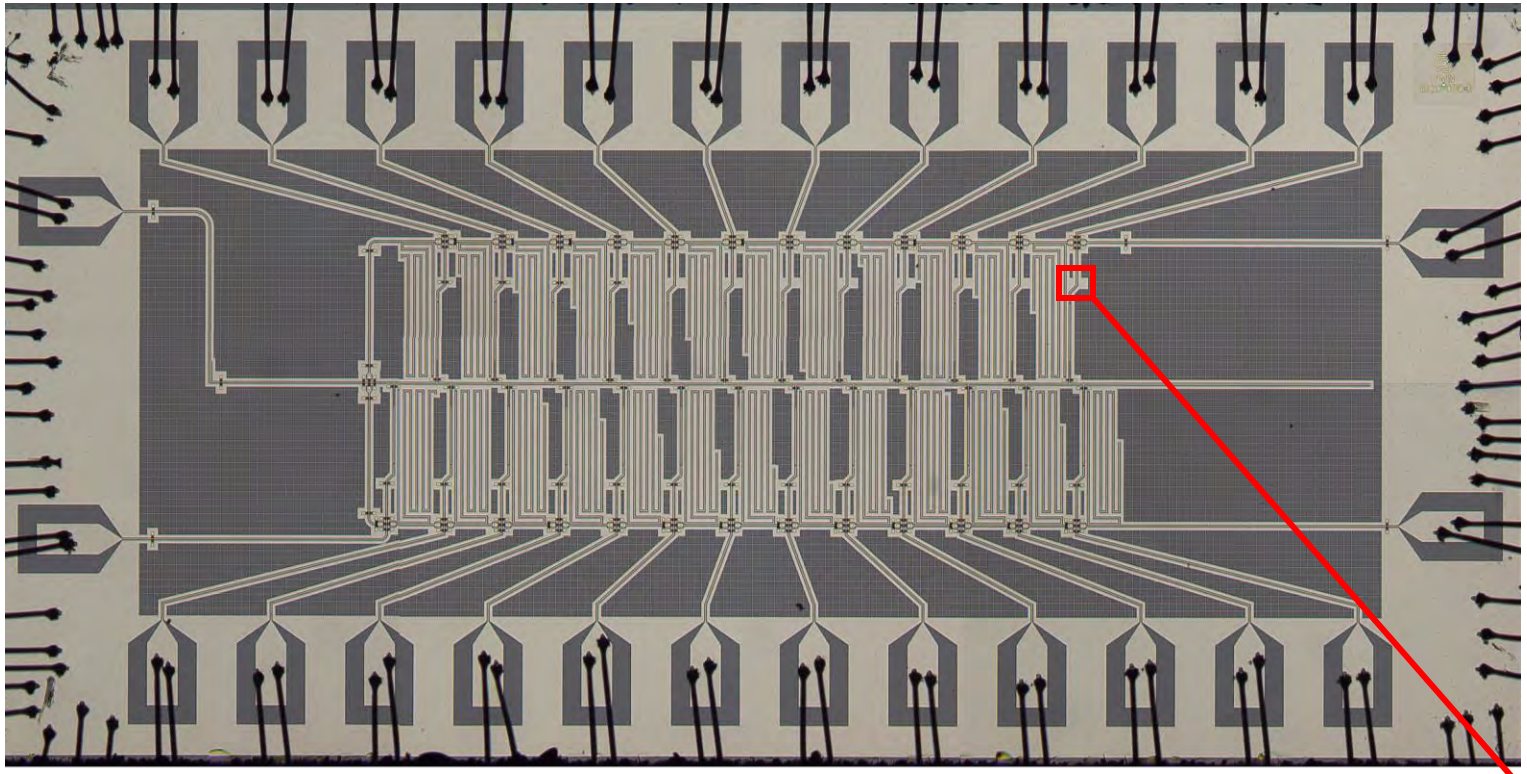

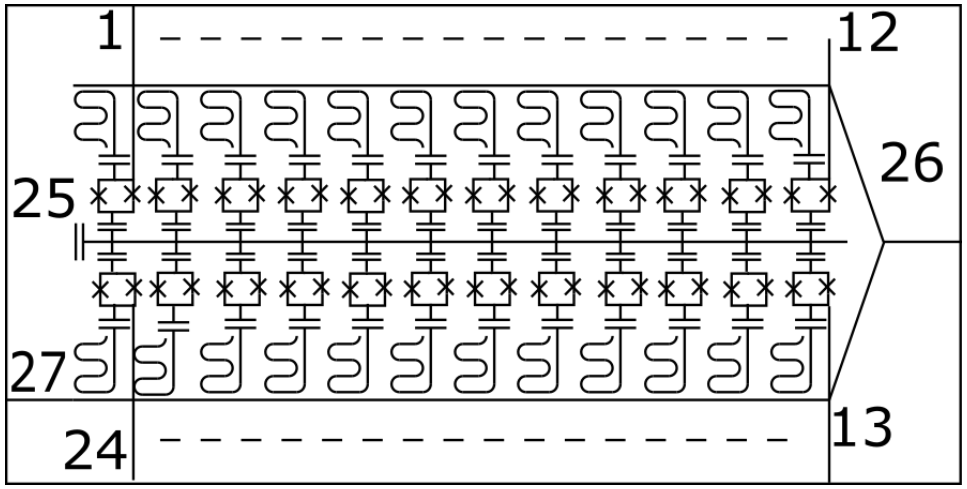

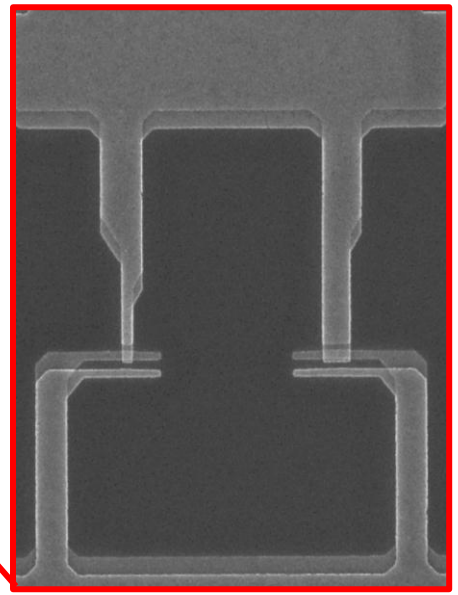

Tavis-Cummings model

$$\hat{H} = \nu_c \, \hat{a}^\dagger \hat{a} + \sum_{j=1}^{N} \epsilon_j \, \hat{\sigma}_j^+ \hat{\sigma}_j^- + \sum_{j=1}^{N} g_j \, (\hat{\sigma}_j^+ \hat{a} + \hat{a}^\dagger \hat{\sigma}_j^-)$$

Array of 25 qubits– Sample holder

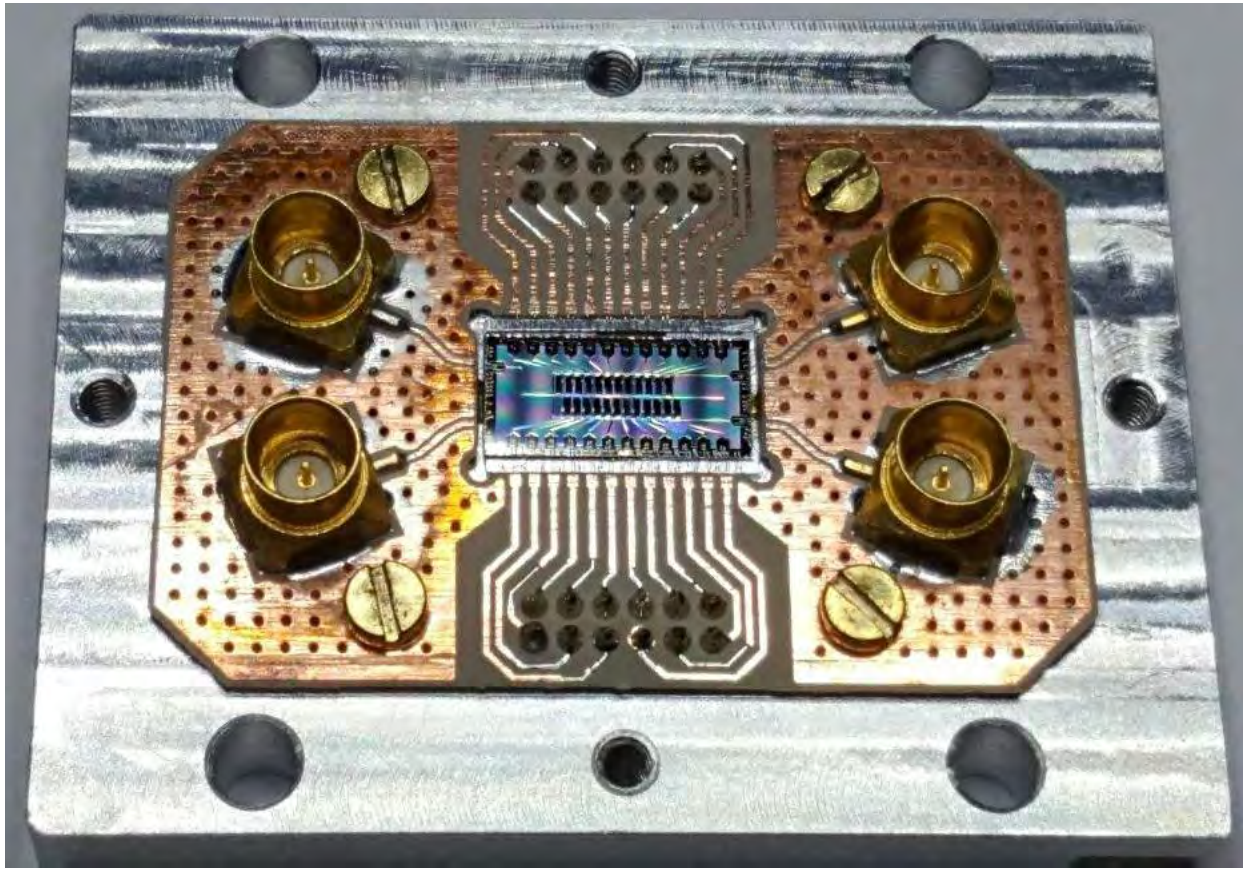

Array of 25 qubits- Description

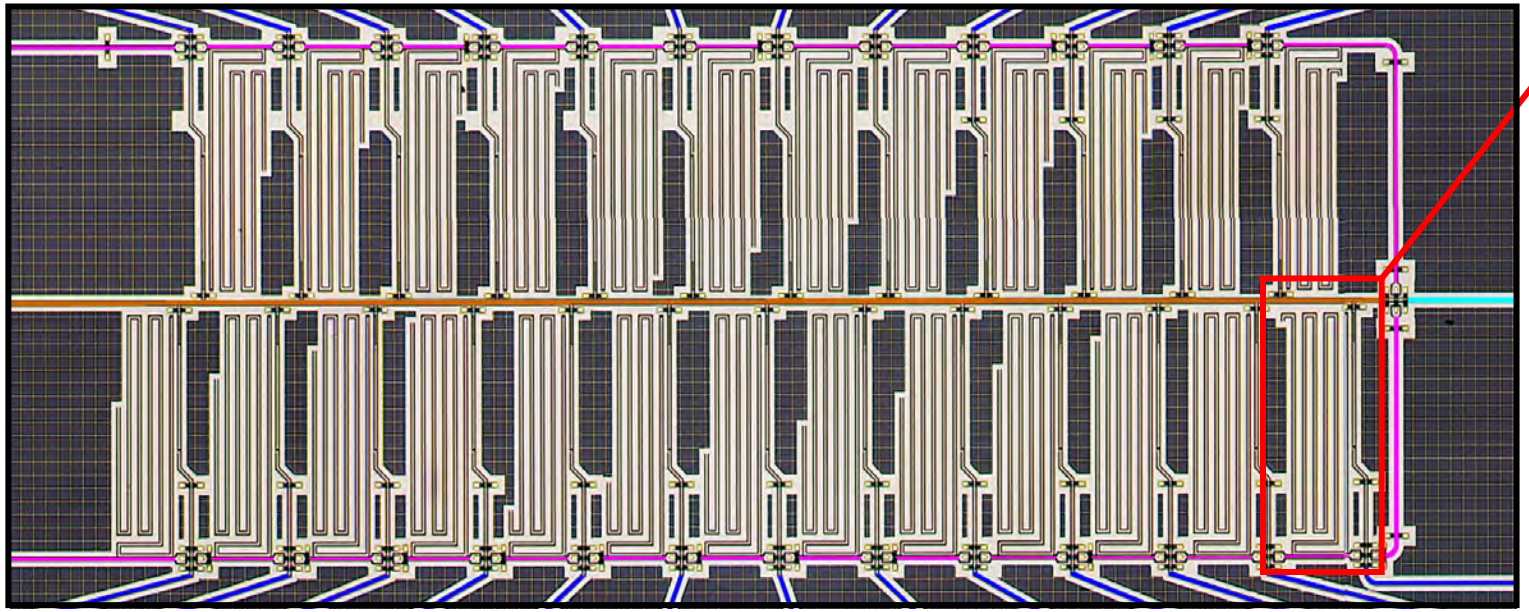

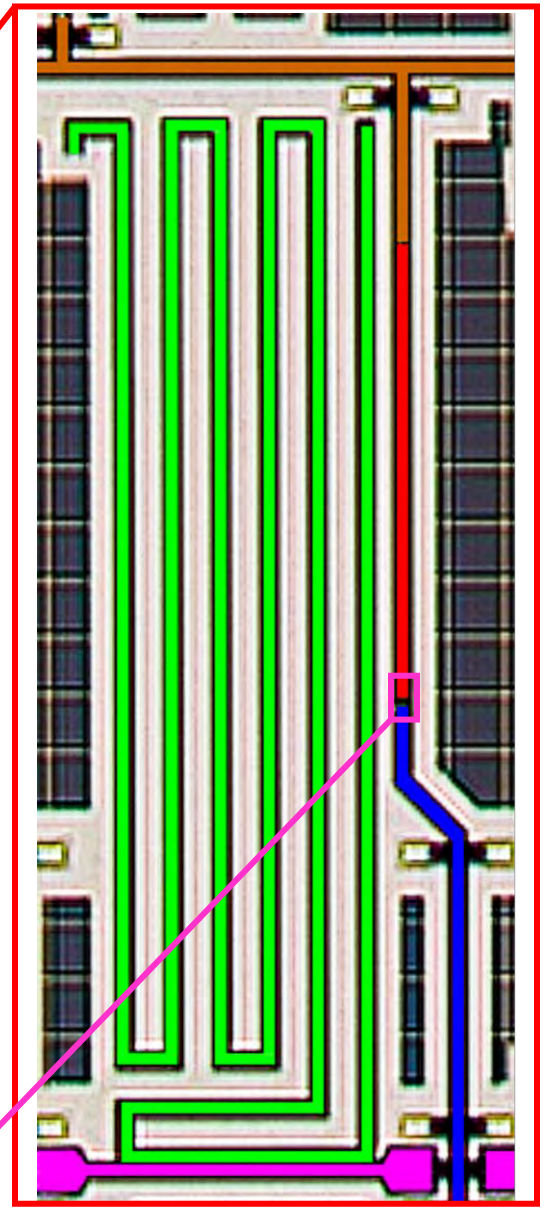

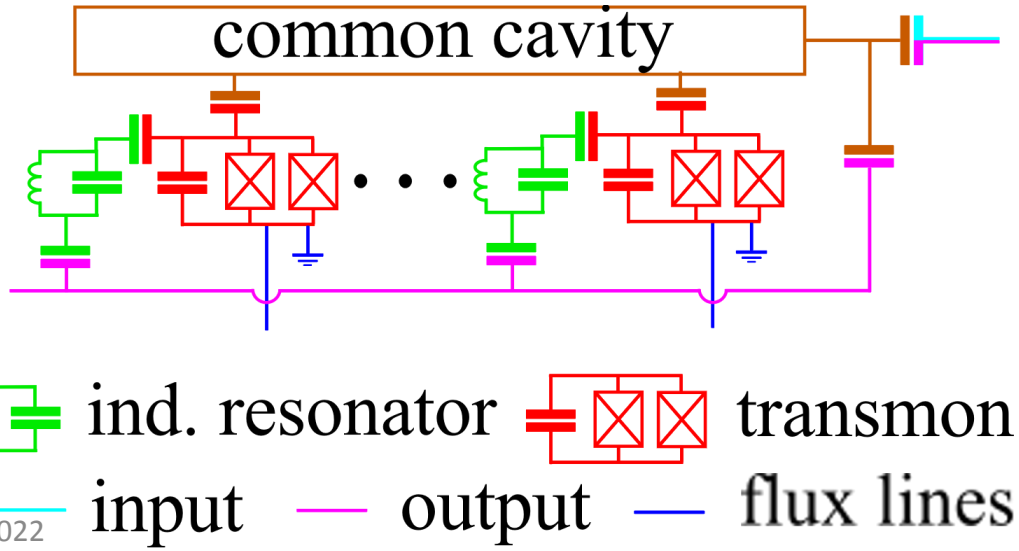

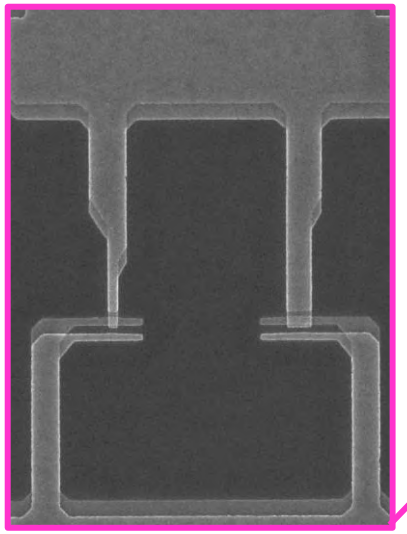

Array of 25 qubits– Set up

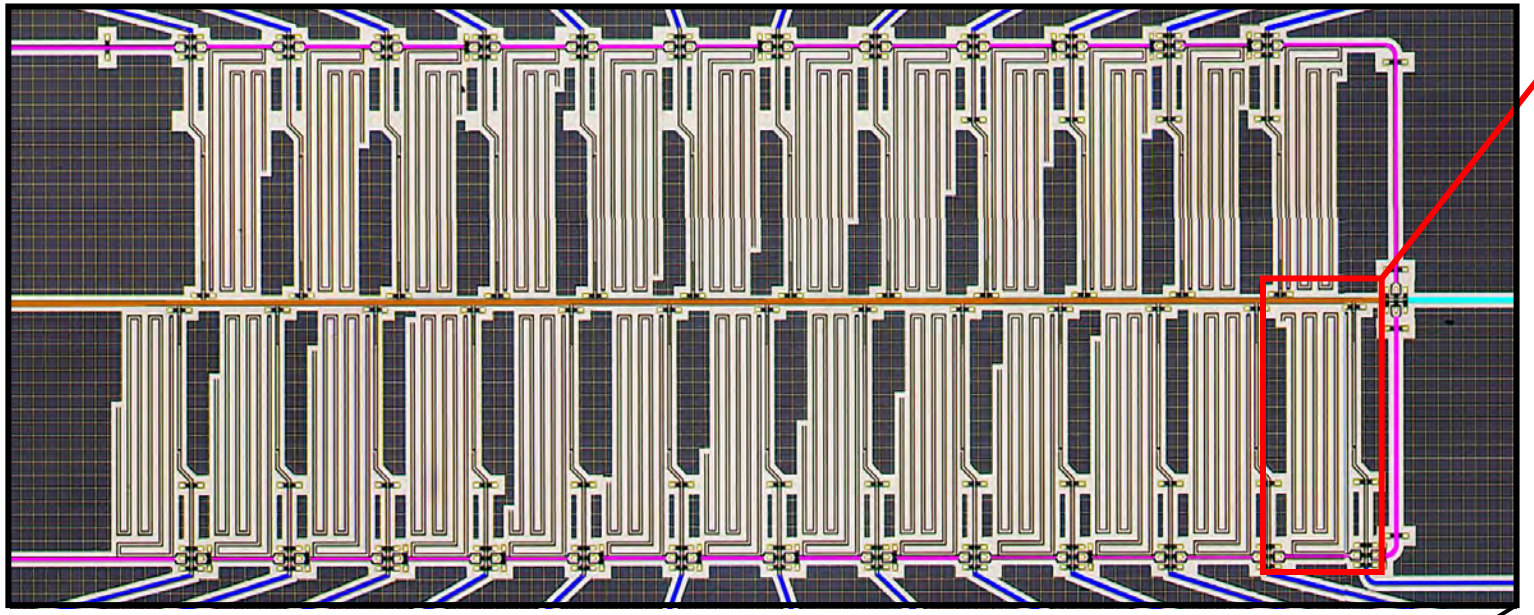

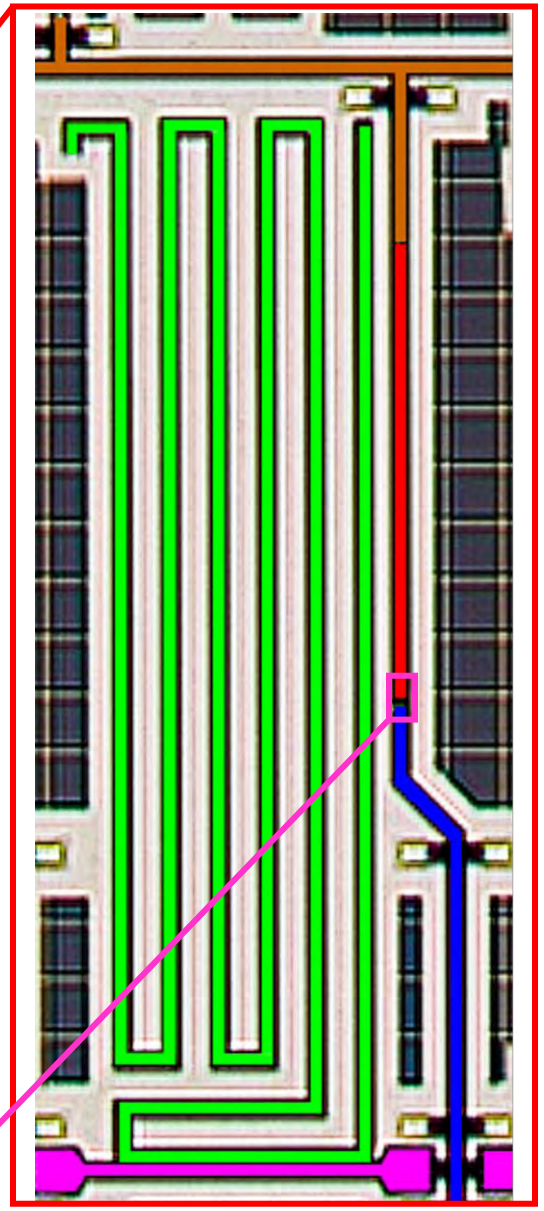

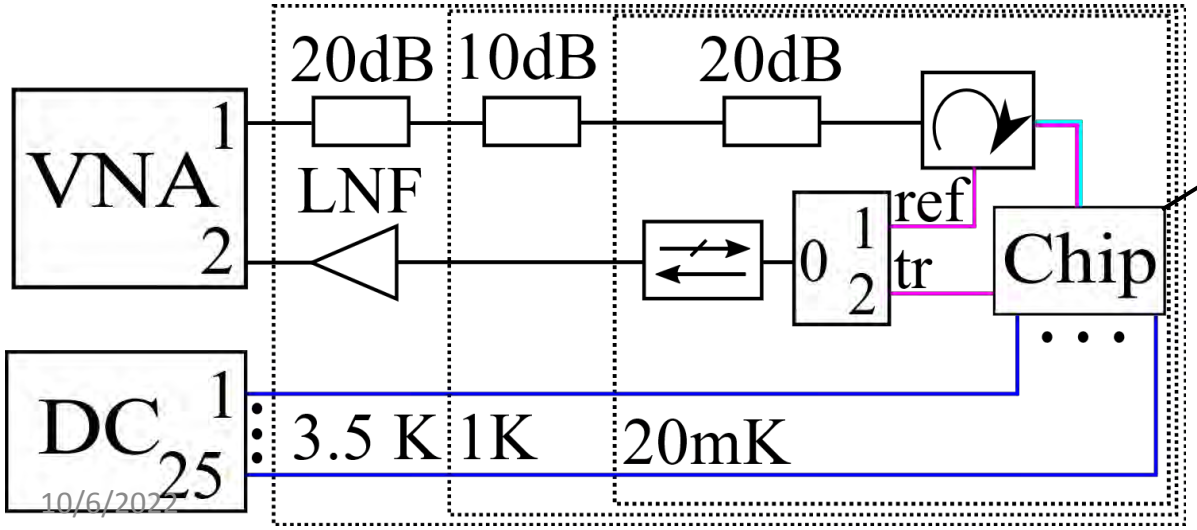

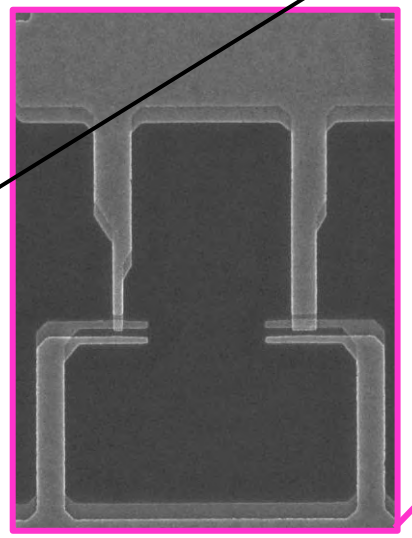

Array of 25 qubits

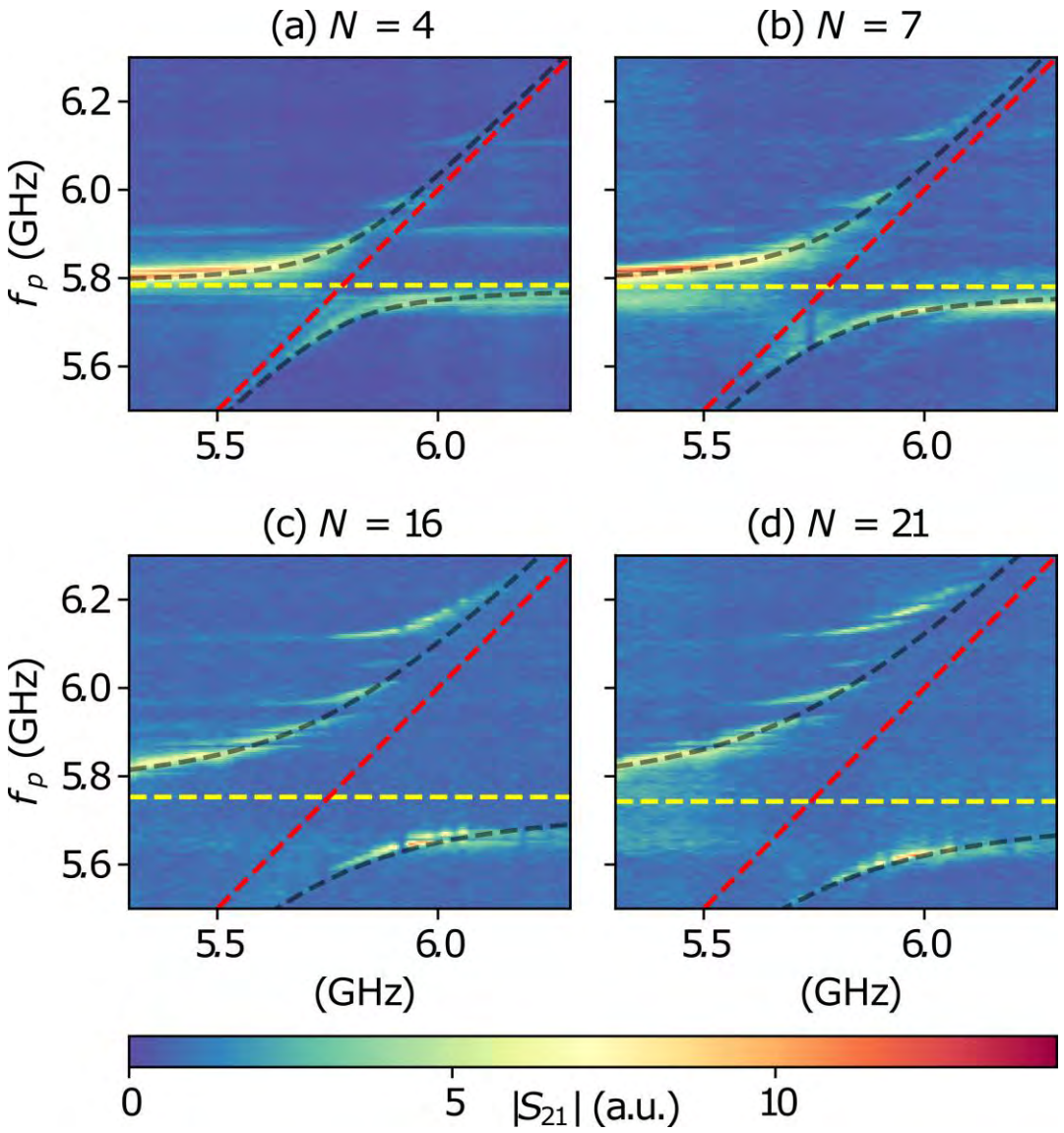

Rabi splitting

$$\Delta = 2g\sqrt{N}$$

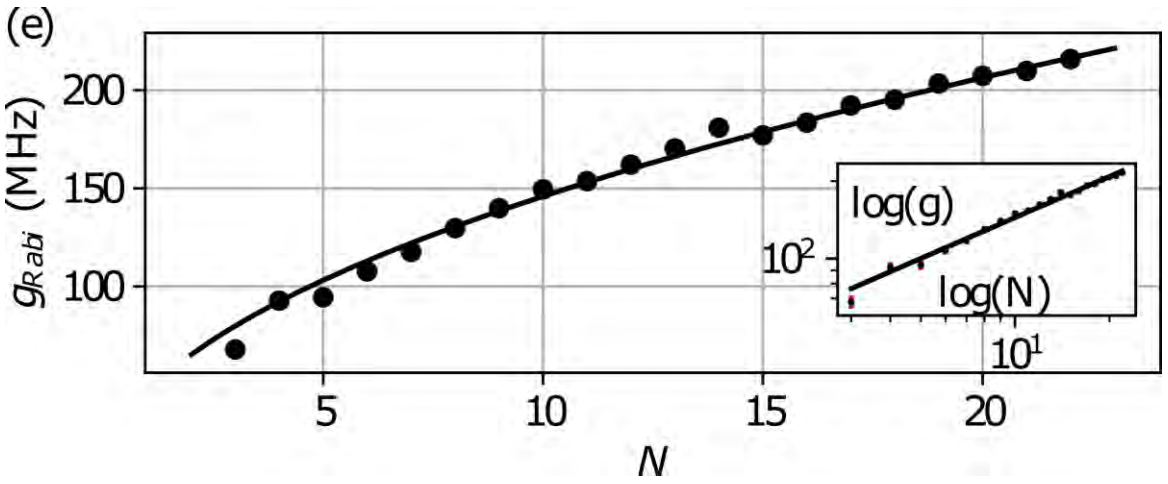

Array of 25 qubits

$$\hat{H} = -\frac{1}{2}h\sum_{i=1}^{N}\hat{\sigma}_z^i\,\varepsilon_i + h\nu_c\hat{a}_c{}^{\dagger}\hat{a}_c + h\sum_{i=1}^{N}g_c^i\left(\hat{a}_c^{i\,\dagger} + \hat{a}_c^i\right)\left(\hat{\sigma}_+^i + \hat{\sigma}_-^i\right) +$$

$$+h\sum_{i=1}^{N}g_{ind}^i\left(\hat{a}_{ind}^{i}{}^{\dagger} + \hat{a}_{ind}^i\right)\left(\hat{\sigma}_+^i + \hat{\sigma}_-^i\right) + h\sum_{i=1}^{N}\nu_{ind}^i\hat{a}_{ind}^{i}{}^{\dagger}\hat{a}_{ind}^i$$

Fluxonium qubit

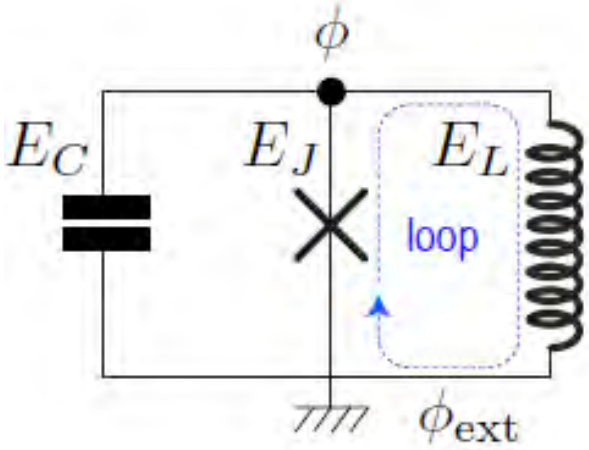

$$E_C < E_J, \quad E_L \ll E_J$$

$$H_F = 4E_C(n)^2 + \frac{E_L}{2}\phi^2 + E_J\left(1 - \cos\left(\phi - {}^{\Phi_{ex}}/_{\Phi_0}\right)\right)$$

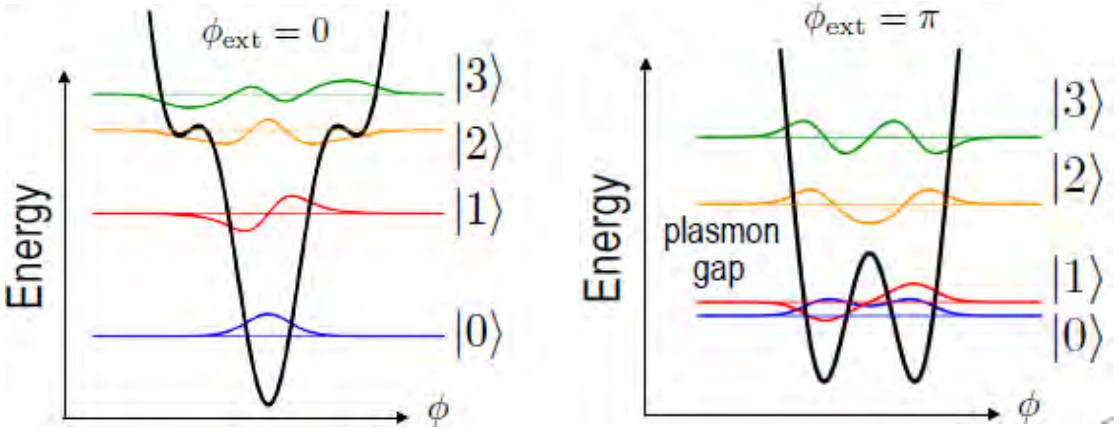

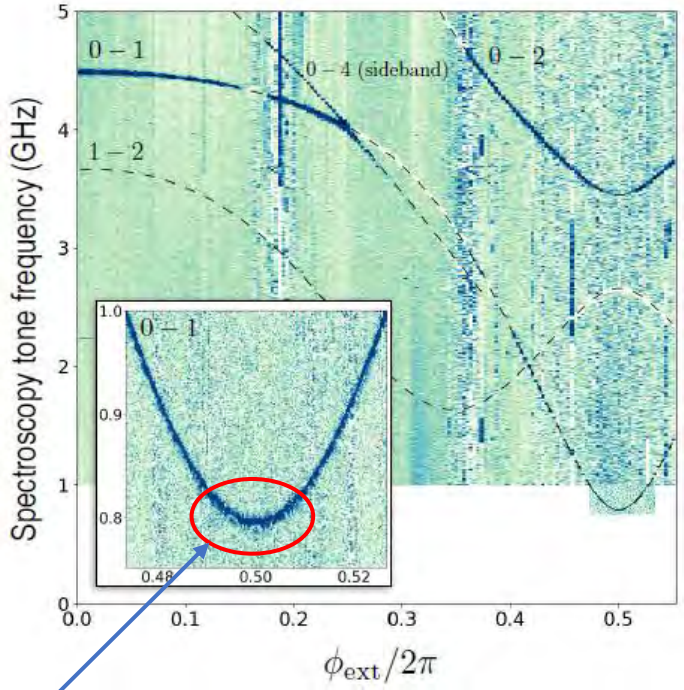

Less than 1GHz

Low dielectric losses

Simpler control system

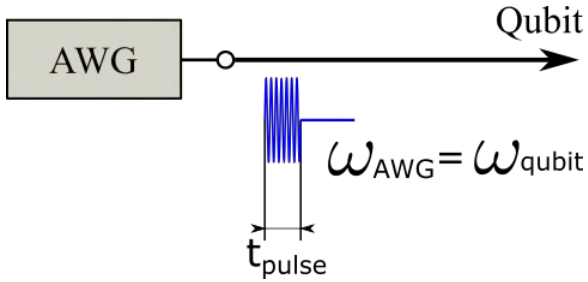

*N. A. Masluk, PhD Thesis at Yale University (2013). **Long B. Nguyen, et al. Phys. Rev. X **9**, 041041

Fluxonium qubit

- Low frequencies (<1000 MHz) -> full qubit control with AWG devices
- Better relaxation T1 > 1 ms *
- Better coherence T2 > 100 us**, best T2 > 1 ms [world record 2021 (F=99.99%)]***
- Two qubit gates in 3D cavities (Fidelity~99.2%) ***
- Two qubit gates on chip (Fidelity~99.6%) *****

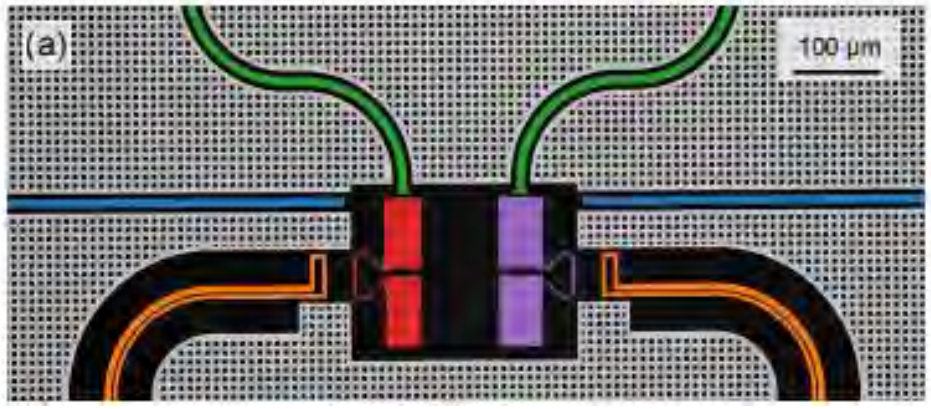

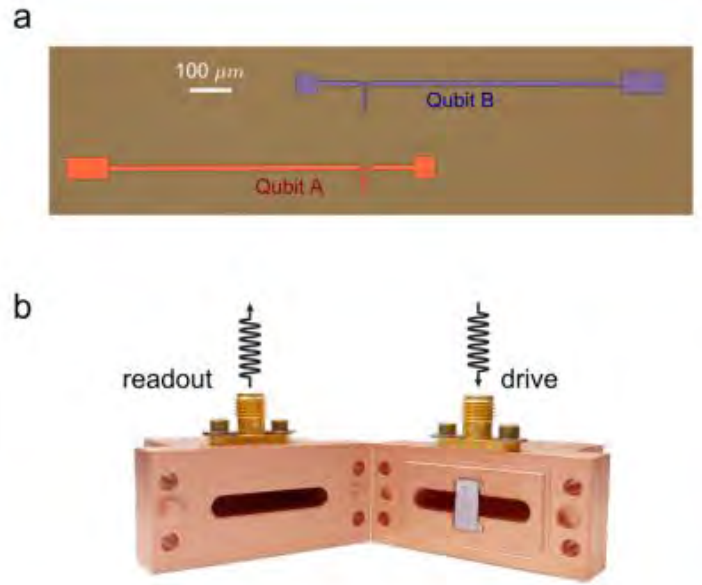

*Ioan M. Pop, et al. *Nature* volume 508, pages369–372(2014)
***https://arxiv.org/abs/2103.08578
***** https://arxiv.org/pdf/2111.13504.pdf

**Long B. Nguyen, et al. Phys. Rev. X 9, 041041
****Quentin Ficheux , et al. Phys. Rev. X **11**, 021026

Two-qubit device with tunable coupling

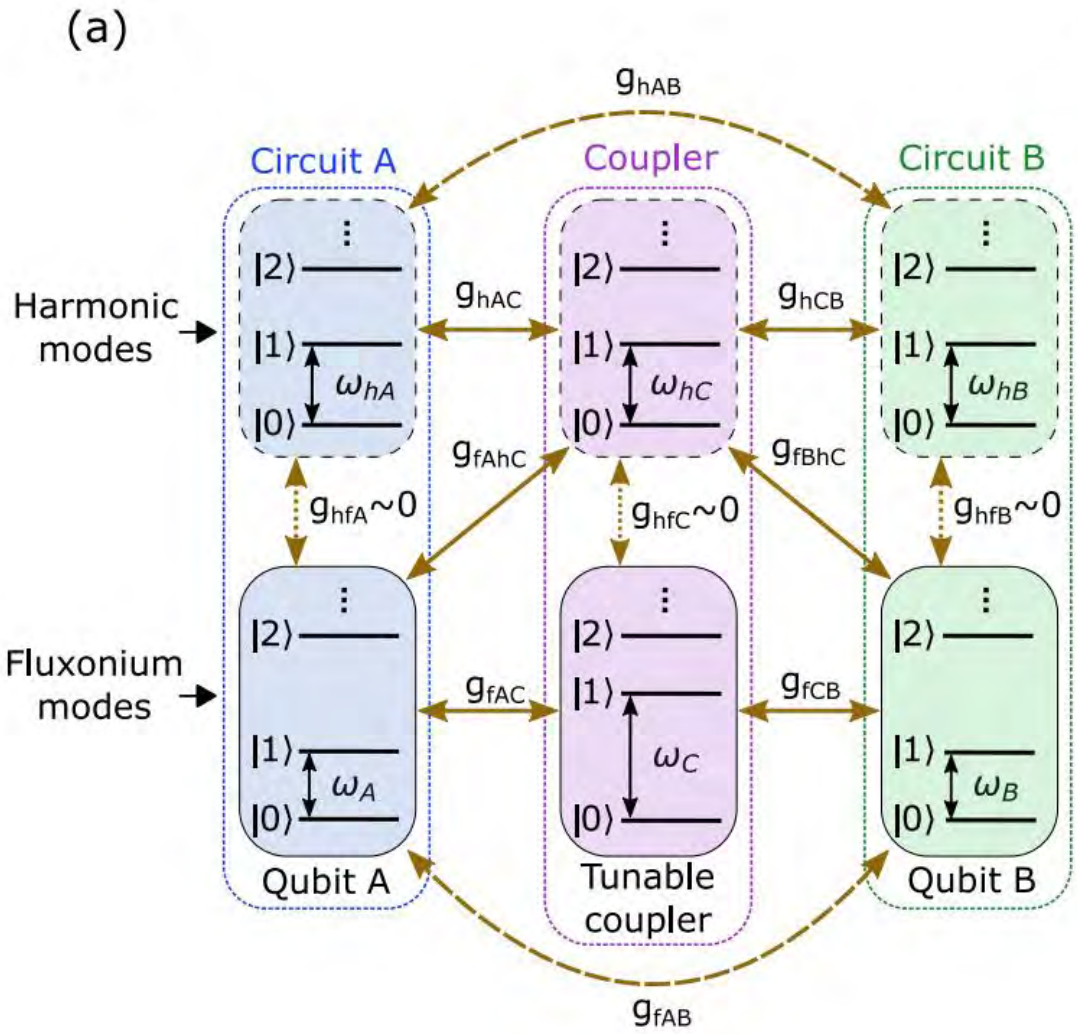

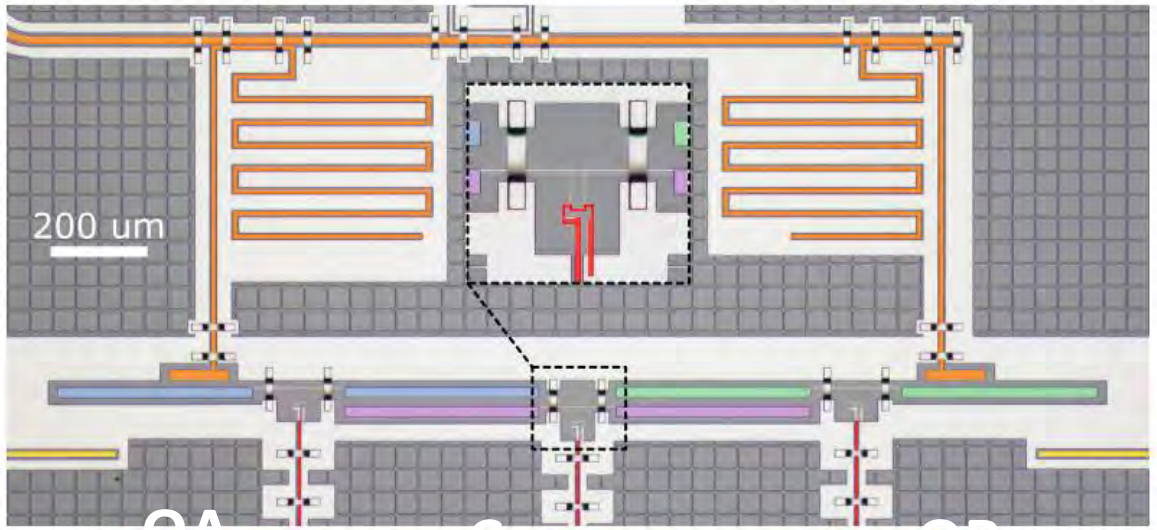

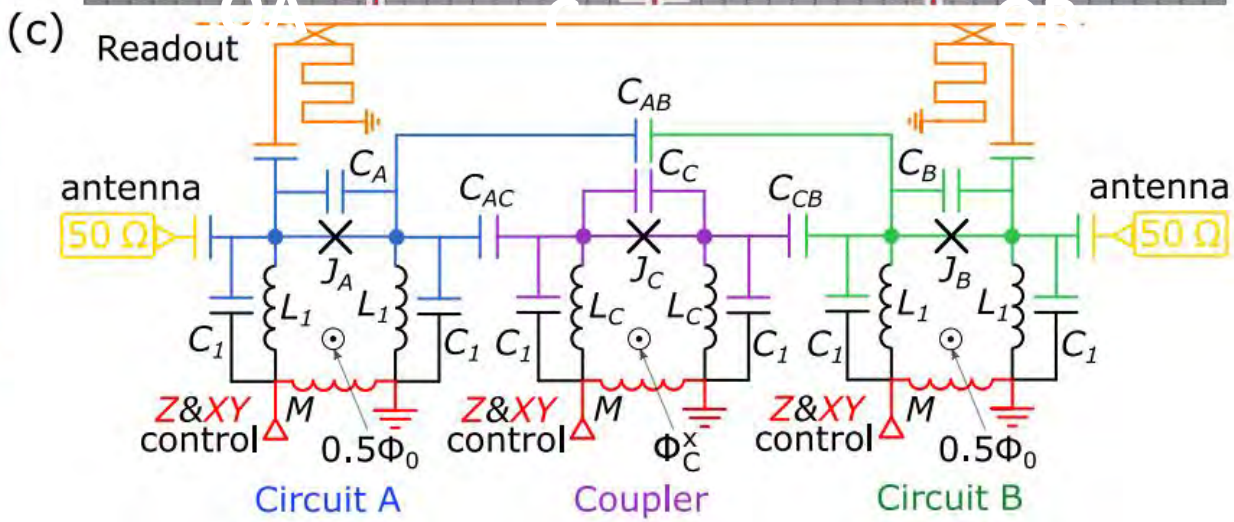

Tunable coupling scheme for implementing two-qubit gates on fluxonium qubits

Cite as: Appl. Phys. Lett. 119, 194001 (2021); https://doi.org/10.1063/5.0064800
Submitted: 27 July 2021 • Accepted: 21 October 2021 • Published Online: 08 November 2021

I. N. Moskalenko, I. S. Besedin, I. A. Simakov, et al.

- Devices were fabricated at the BMSTU Nanofabrication Facility (Functional Micro/Nanosystems)

Device parameters and coherent properties

TABLE I. Device parameters

Parameter	Qubit A	Qubit B	Qubit S
E_{Ch} (GHz)	0.562	0.562	0.568
E_{Cf} (GHz)	0.567	0.567	0.564
E_{L} (GHz)	0.835	0.835	0.858
E_{J} (GHz)	2.052	2.061	1.989
$\omega_{10}^{\mathrm{f}}/2\pi$ (MHz)	688.224	664.763	750.123
$\omega_{12}^{\mathrm{f}}/2\pi$ (GHz)	1.832	1.835	1.803
$\omega_{10}^{\mathrm{h}}/2\pi$ (GHz)	1.940	1.940	2.006
T_1 (μs)	87	86	172
T_2^* (μs)	51	76	113
T_2^E (μs)	107	93	146
$\omega_r/2\pi$ (GHz)	7.167	7.383	6.841
$\kappa_r/2\pi$ (MHz)	7.6	7.2	7.4
$\chi_r/2\pi$ (MHz)	0.257	0.272	0.495

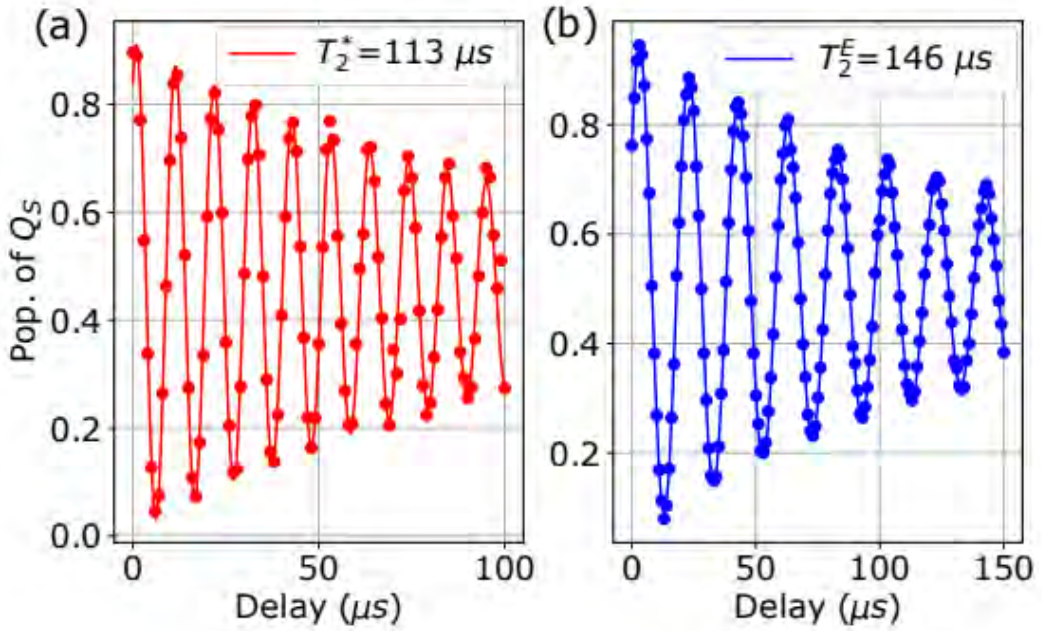

Device parameters and coherent properties

TABLE I. Device parameters

Parameter	Qubit A	Qubit B	Qubit S
E_{Ch} (GHz)	0.562	0.562	0.568
E_{Cf} (GHz)	0.567	0.567	0.564
E_{L} (GHz)	0.835	0.835	0.858
E_{J} (GHz)	2.052	2.061	1.989
$\omega_{10}^{\mathrm{f}}/2\pi$ (MHz)	688.224	664.763	750.123
$\omega_{12}^{\mathrm{f}}/2\pi$ (GHz)	1.832	1.835	1.803
$\omega_{10}^{\mathrm{h}}/2\pi$ (GHz)	1.940	1.940	2.006
T_1 (μs)	87	86	172
T_2^* (μs)	51	76	113
T_2^E (μs)	107	93	146
$\omega_r/2\pi$ (GHz)	7.167	7.383	6.841
$\kappa_r/2\pi$ (MHz)	7.6	7.2	7.4
$\chi_r/2\pi$ (MHz)	0.257	0.272	0.495

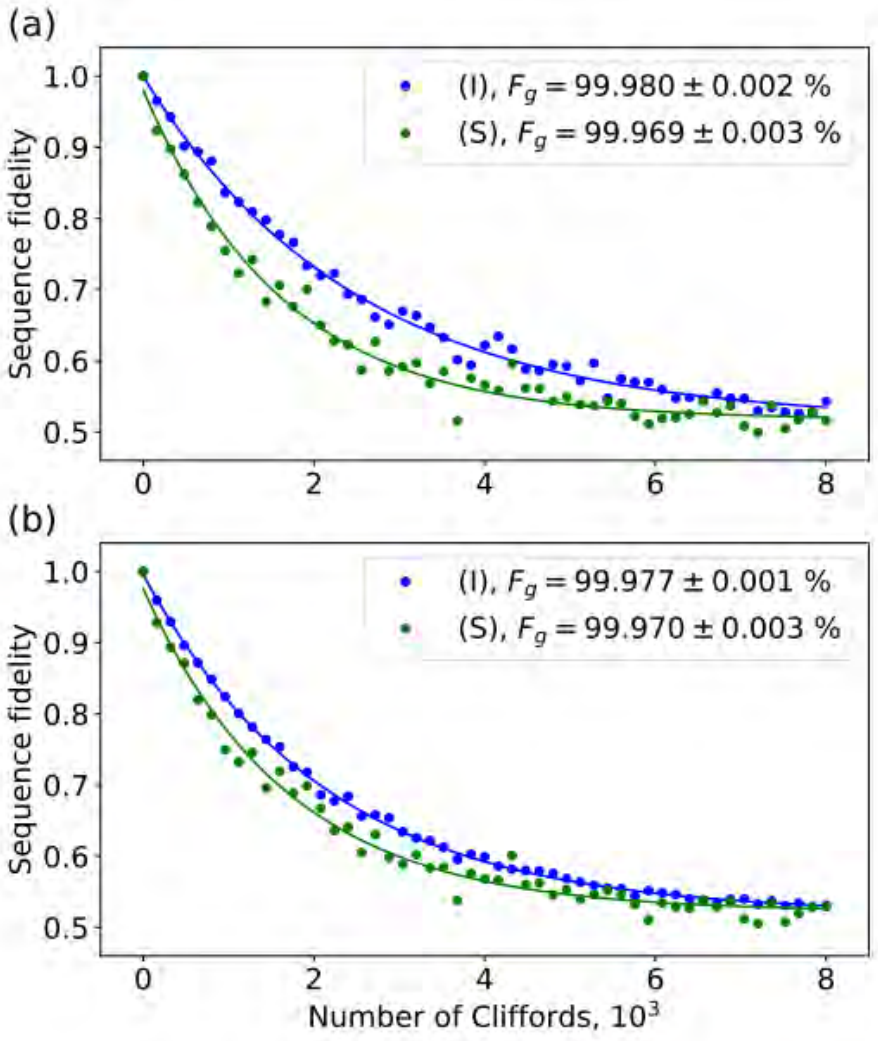

Length = 13.3 ns

Sigma = 3.325 ns

α ~ -1.8

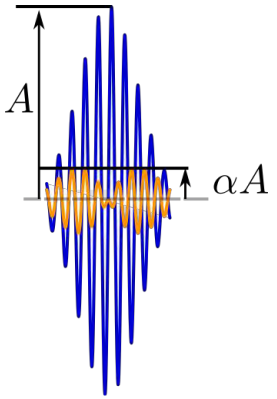

Cross-entropy benchmarking (XEB) with fSim gate

$$U_{\mathrm{fSim}} = \begin{pmatrix} 1 & 0 & 0 & 0 \\ 0 & \cos\theta & -i\sin\theta & 0 \\ 0 & -i\sin\theta & \cos\theta & 0 \\ 0 & 0 & 0 & e^{-i\varphi} \end{pmatrix}$$

$$\theta/\pi = -0.2502 \quad \varphi/\pi = 0.0255$$

$$U_{\mathrm{fSim}} = \begin{pmatrix} 1 & 0 & 0 & 0 \\ 0 & \frac{\sqrt{2}}{2}e^{i\varphi_1} & i\frac{\sqrt{2}}{2}e^{i(\varphi_1-\varphi_2+\varphi_3)} & 0 \\ 0 & -i\frac{\sqrt{2}}{2}e^{i(\varphi_1-\varphi_2+\varphi_3)} & \frac{\sqrt{2}}{2}e^{i\varphi_2} & 0 \\ 0 & 0 & 0 & e^{-i(\varphi+\varphi_1+\varphi_2)} \end{pmatrix}$$

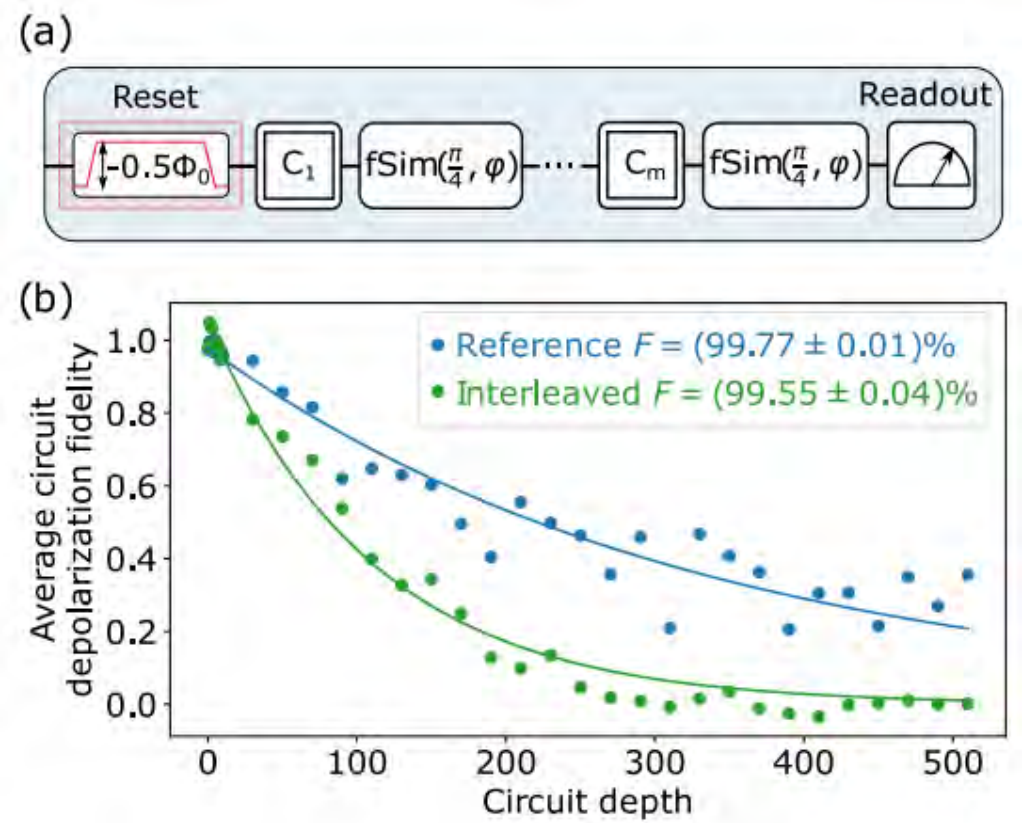

100 random sequences for each circuit depth (m)

*https://quantumai.google/cirq/qcvv/xeb_theory

* arXiv:2203.16302v2

CZ gate calibration

Ising ZZ gate

Ising XX gate (up to 1-qubit Rz)

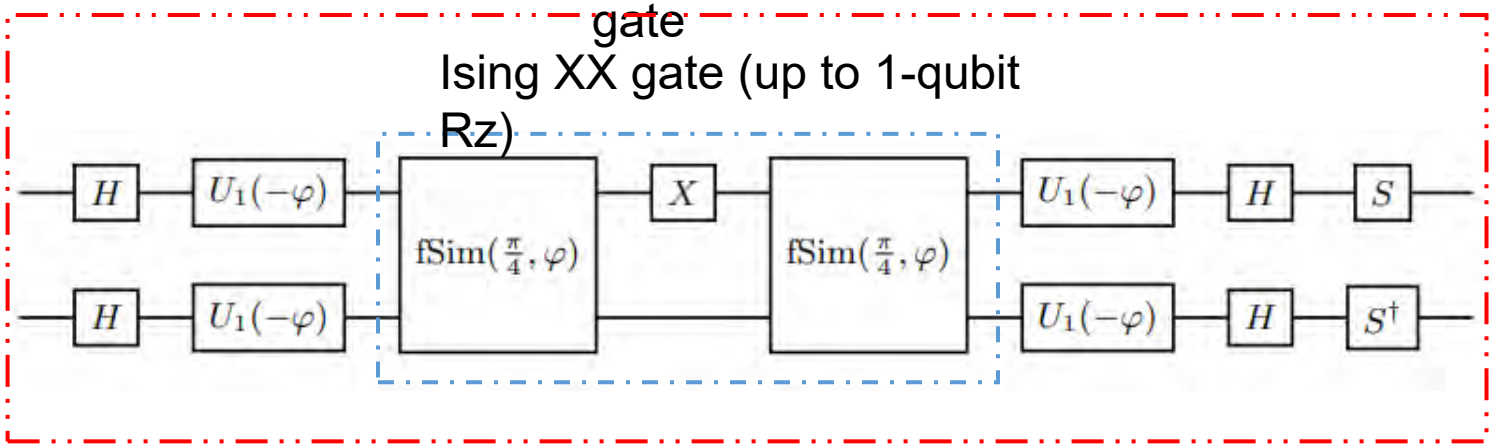

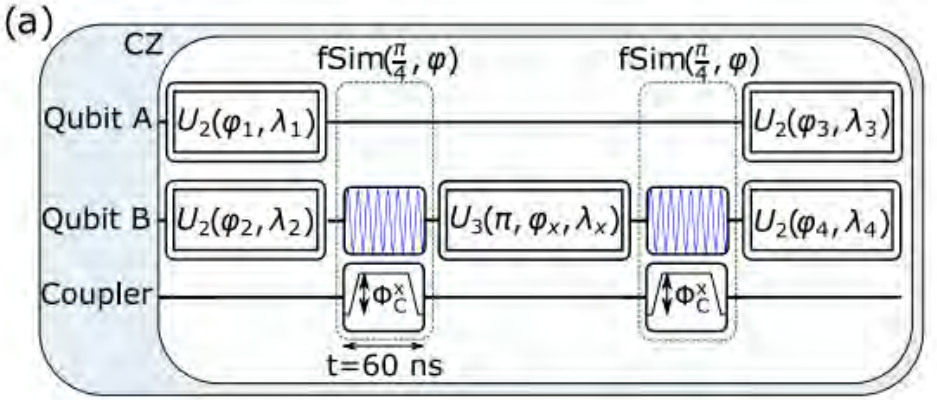

CZ gate tomography

99.4%

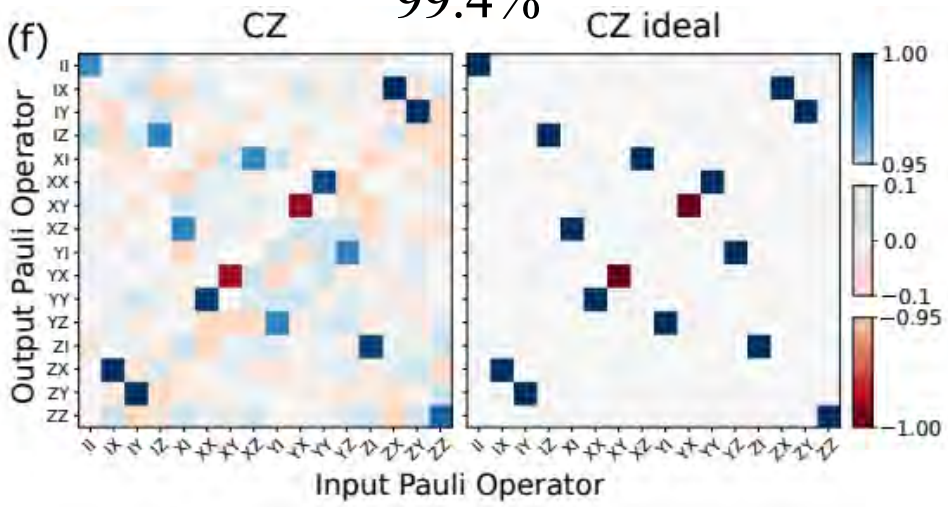

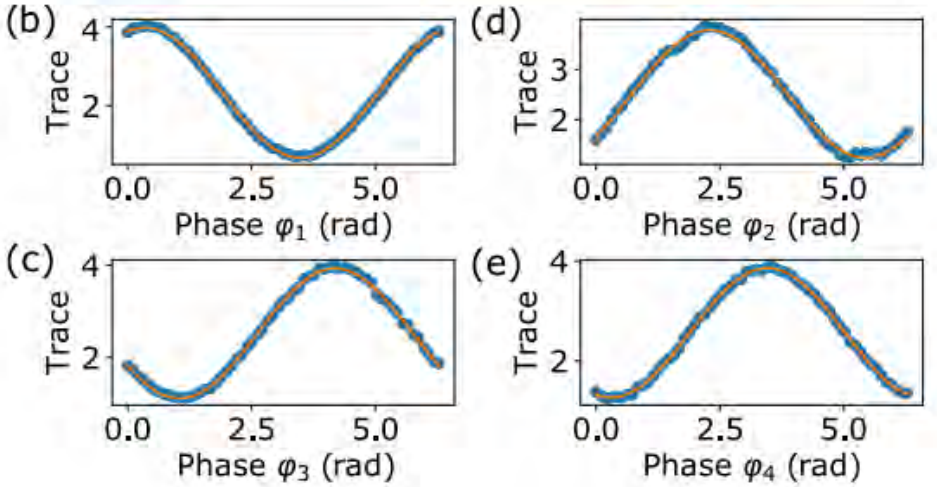

* arXiv:2203.16302v2

XEB with CZ gate

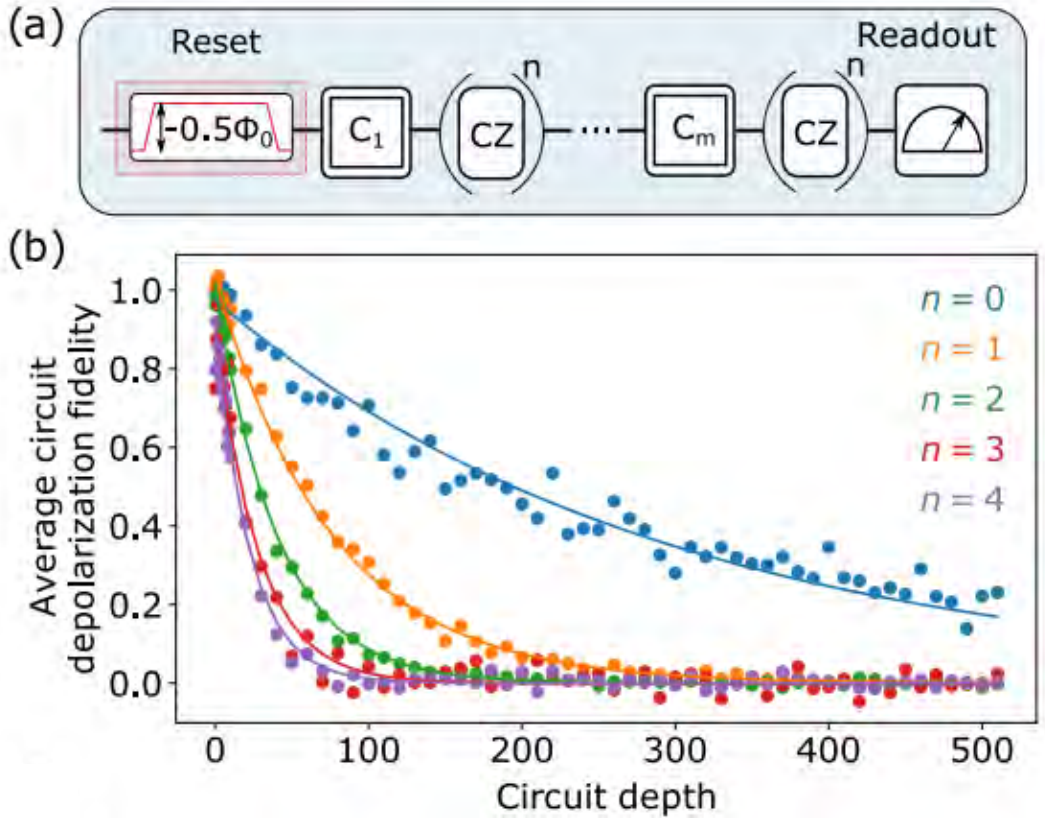

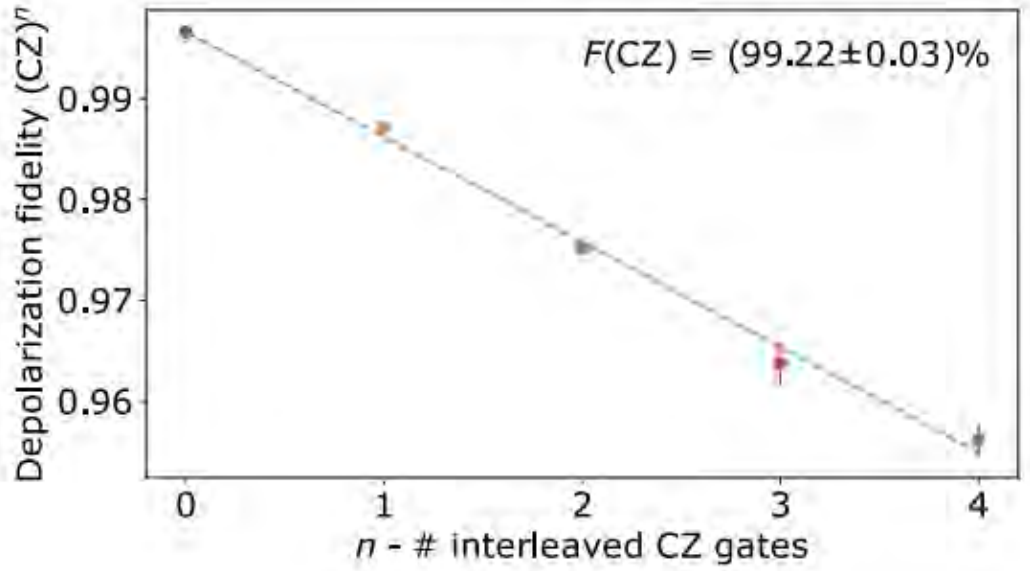

100 random sequences for each circuit depth (m)

* arXiv:2203.16302v2

Conclusion

- Chain of 11 qubits
  - Single-photon topological states
  - Two-photon bound states

- Array of 25 qubits
  - Rabi splitting and mesoscopic fluctuations

- On-chip fluxonium qubits are developed
  - Single-qubit gate fidelities are better than 99.97 %
  - Two-qubit fSim gate fidelity about 99.55 %
  - Two-qubit CZ gate fidelity about 99.23 %

This work was implemented by

Research team (MISiS subgroup):

Aleksey Ustinov
Valery Ryazanov
Ilya Besedin
Ilya Moskalenko
Nikolay Abramov
Ilya Simakov
Elena Egorova
Grigoriy Mazhorin
Alexey Vasiliev
Alena Kazmina
Vladimir Chichkov
Tanya Kim
Sasha Grigoriev

Technology (BMSTU):

Ilia Rodionov

Alina Dobronosova
Dmitriy Moskalev
Anastasya Pishimova

Thank you for your attention

Qubit control

Transmon

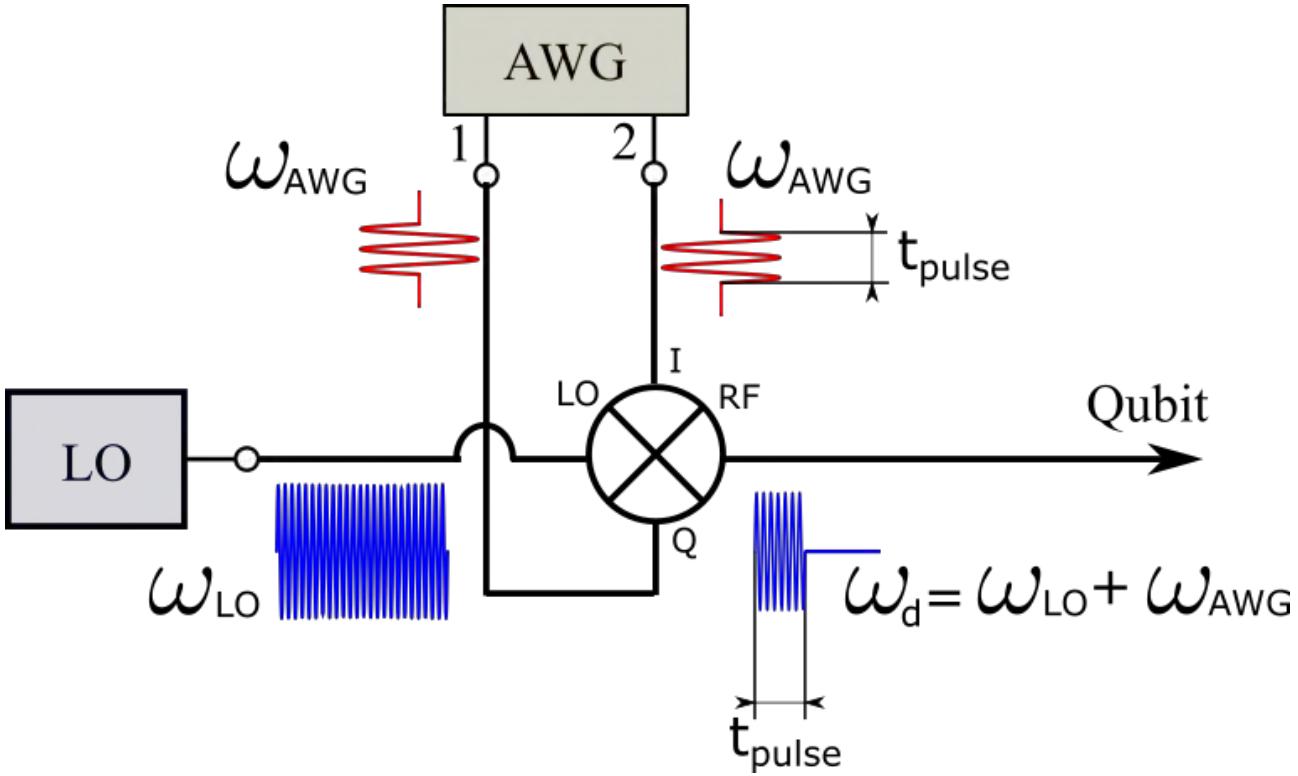

Chain of 11 qubits – Results

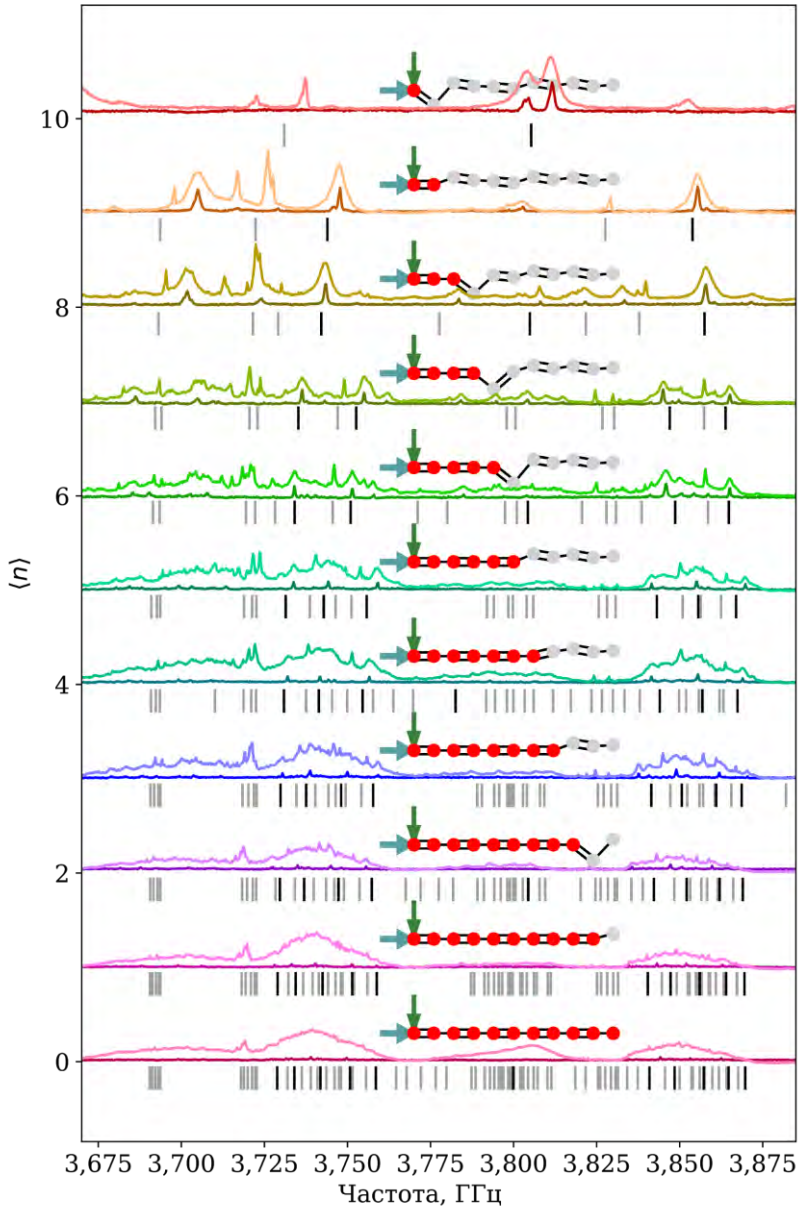

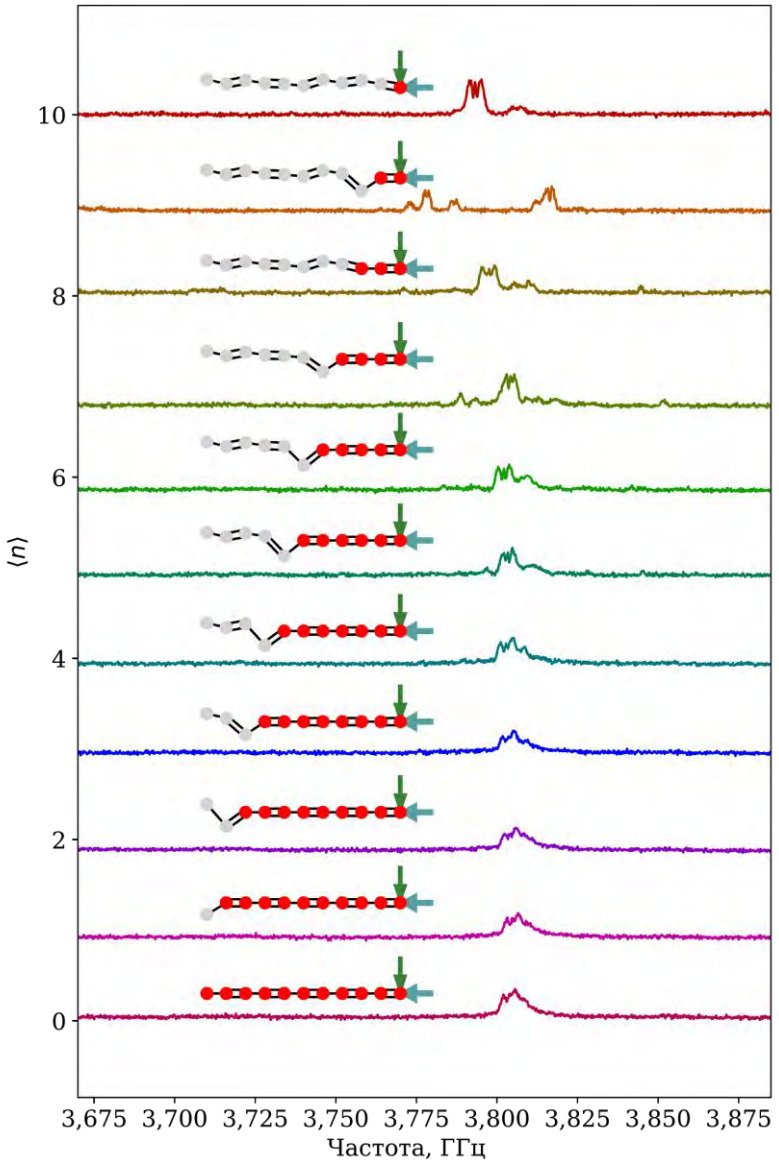

Chain of 11 qubits – Results

q	f_r, GHz	$L_{q,q-1}, V/\Phi_0$	$L_{q,q}, V/\Phi_0$	$L_{q,q+1}, V/\Phi_0$	$\Phi_q^{(0)}, \Phi_0$	E_{qJ1}, GHz	E_{qJ2}, GHz
1	6.260		-0.1121	-0.0005	0.1672	11.816	1.944
2	6.307	0.0008	-0.1128	-0.0001	0.1127	11.168	1.673
3	6.362	0.0006	-0.1119	-0.0006	0.1305	11.815	1.911
4	6.414	0.0004	-0.1120	-0.0003	0.0936	11.263	1.769
5	6.459	0.0006	-0.1129	-0.0017	0.1193	10.981	1.811
6	6.498	0.0003	-0.1103	-0.0003	0.1103	10.909	1.608
7	6.555	0.0003	-0.1053	-0.0022	0.1237	11.666	1.989
8	6.606	0.0007	-0.1057	-0.0005	0.1235	10.903	2.189
9	6.658	0.0003	-0.1097	-0.0017	0.1060	11.563	2.001
10	6.711	0.0001	-0.1047	-0.0005	0.0640	11.045	1.941
11	6.763	0.0005	-0.1074		0.0756	11.265	1.946

Array of 25 qubits- Calibrations

$$\varepsilon(\phi) = \sqrt{8E_C}\left((E_{J1}+E_{J2})^2\cos^2\phi + (E_{J1}-E_{J2})^2\sin^2\phi\right)^{\frac{1}{4}} - E_C$$

$$\phi_i = \sum L_{ij}V_j + \phi_i^0$$

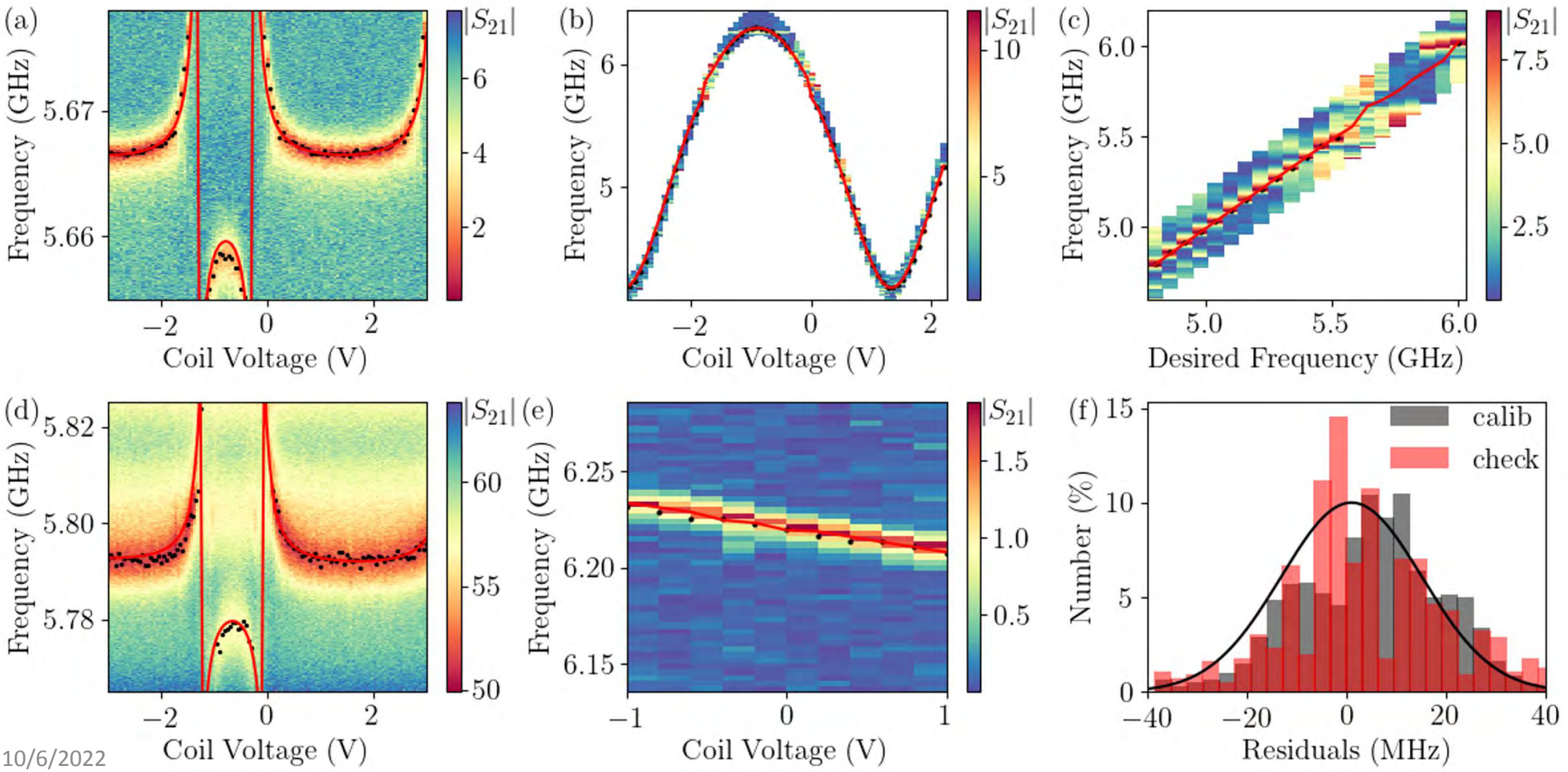

Array of 25 qubits- Random frequency sets

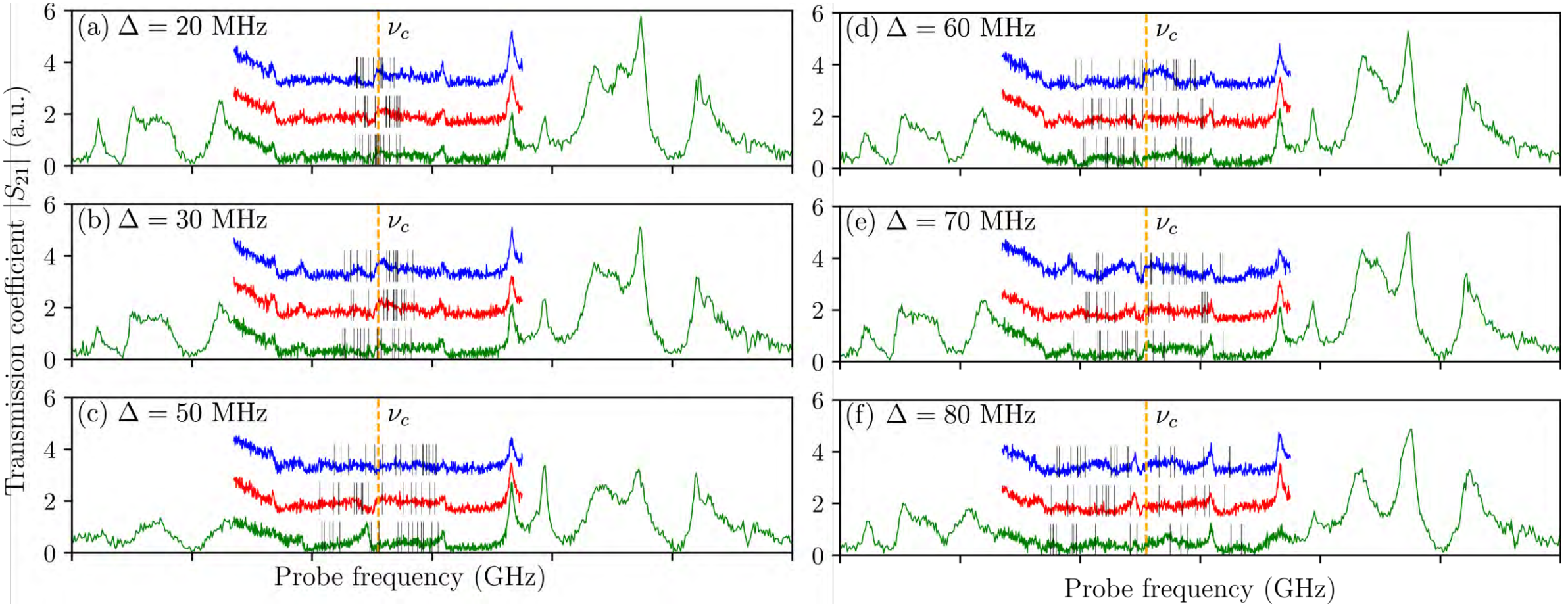

Array of 25 qubits– Mesoscopic fluctuations

$$\langle S_{21}\rangle = \sqrt{\gamma_{\text{in}}\gamma_{\text{out}}}\frac{-i}{\kappa + \pi g^2 N/\Delta} \qquad \langle|\delta S_{21}|^2\rangle = \gamma_{\text{in}}\gamma_{\text{out}}\frac{g^4}{(\kappa + \pi g^2 N/\Delta)^4}\frac{\pi N}{2\Gamma\Delta}$$

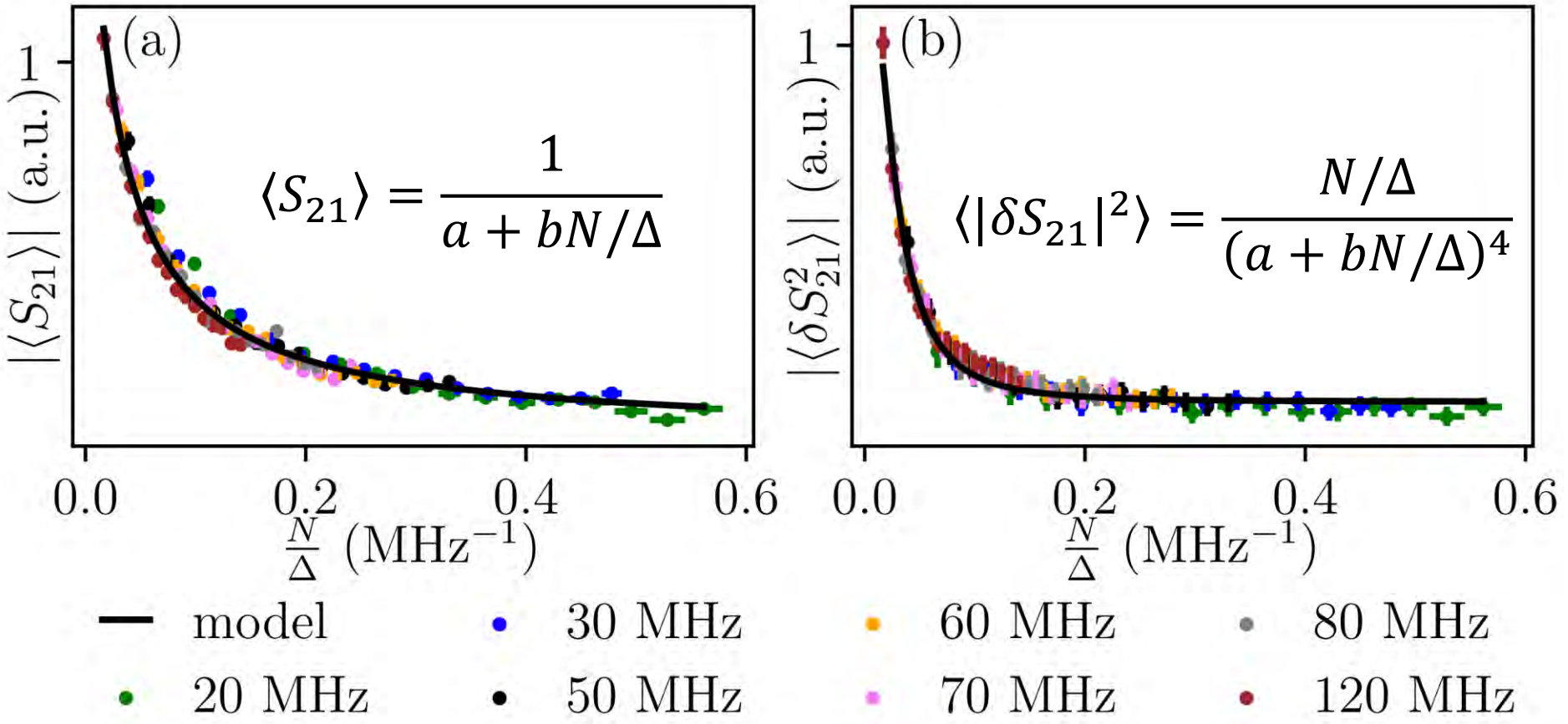

Reduce the environmental noise

Replacing niobium with tantalum

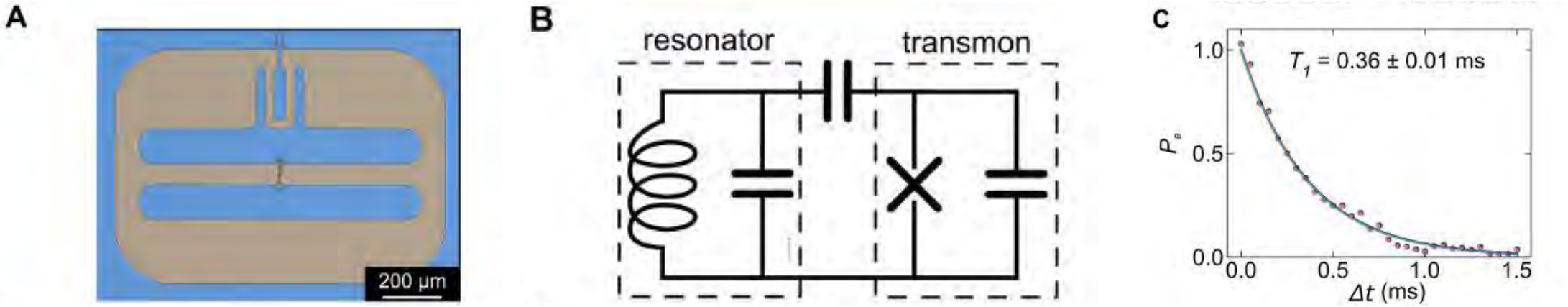

$T_1 = 0.36\ ms$
$T_2 = 0.3\ ms$

The same technology for fluxonium

$T_1 = 1.9\ ms$

Place, A.P.M., *et al. Nat Commun* **12**, 1779 (2021). https://doi.org/10.1038/s41467-021-22030-5

Modern Transmon qubits

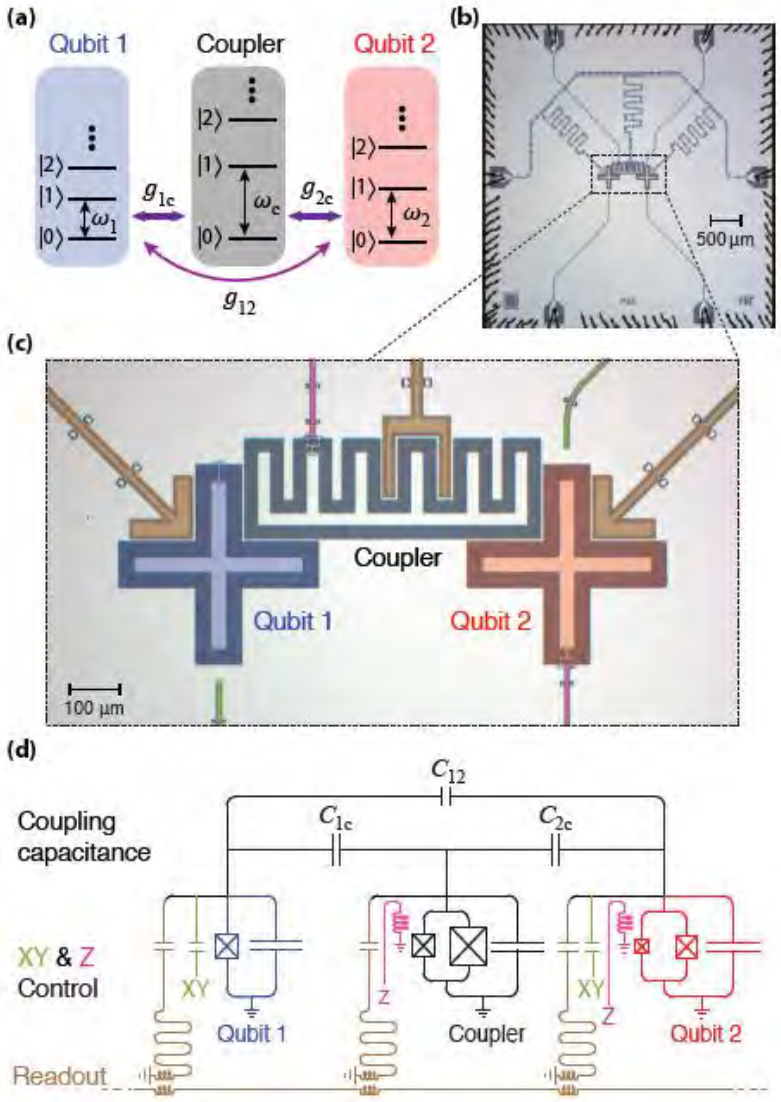

Transmon qubits

- Transmon qubits are easier to design, fabricate and calibrate
- High fidelity two-qubit gates (CZ, CNOT, $\sqrt{\text{iSWAP}}$; $F > 99\%$)

- Good coherence properties (but it could be better)

- High frequency (need IQ-mixers)
- Low anharmonicity
- High dielectric losses

Experimental setup

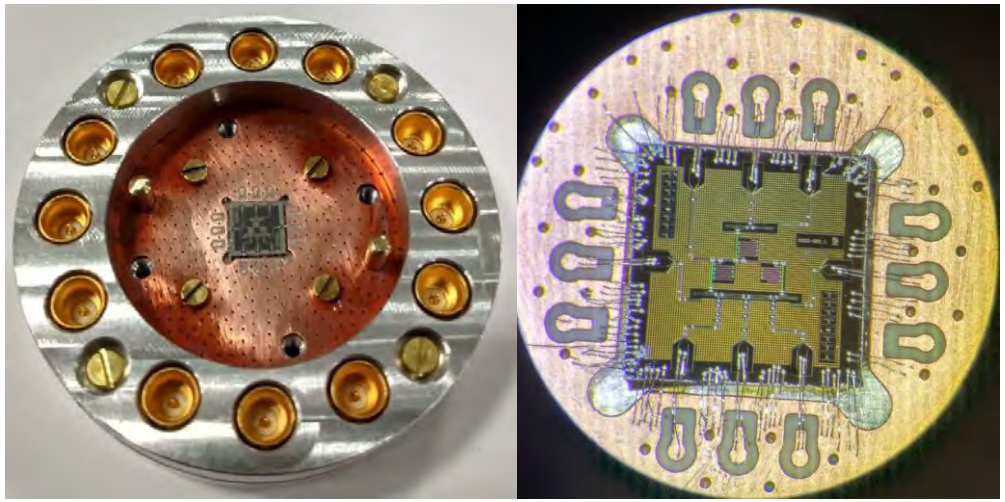

VNA ch2 ch1 — R&S ZVB20 vector network analyser

DIG — Texas instruments ADS54j40/TSW14j56 digitizer

Yokogawa GS200

LO — Agilent E8257D signal generator

AWG — Zurich instruments HDAWG8 arbitrary waveform generator

SA — Agilent N9030A spectrum analyzer

Raditec RADC-4.0-8.0-Cryo circulator

Quinstar CWJ1019KS414 isolator

Superconducting MW lines

MW lines

Mini-Circuits ZX10-2-183-S+ splitter

Mikran 16 dB directional coupler

Marki IQ0318L mixer

Attenuator

PF — Powder Filter (PF)

25 dB — Mini-Circuits ZVA-183-S+ amplifier

HEMT — LNF-LNC0.3_14A amplifier

IMPA — Parametric amplifier

LP — Low-Pass Filter (LP)
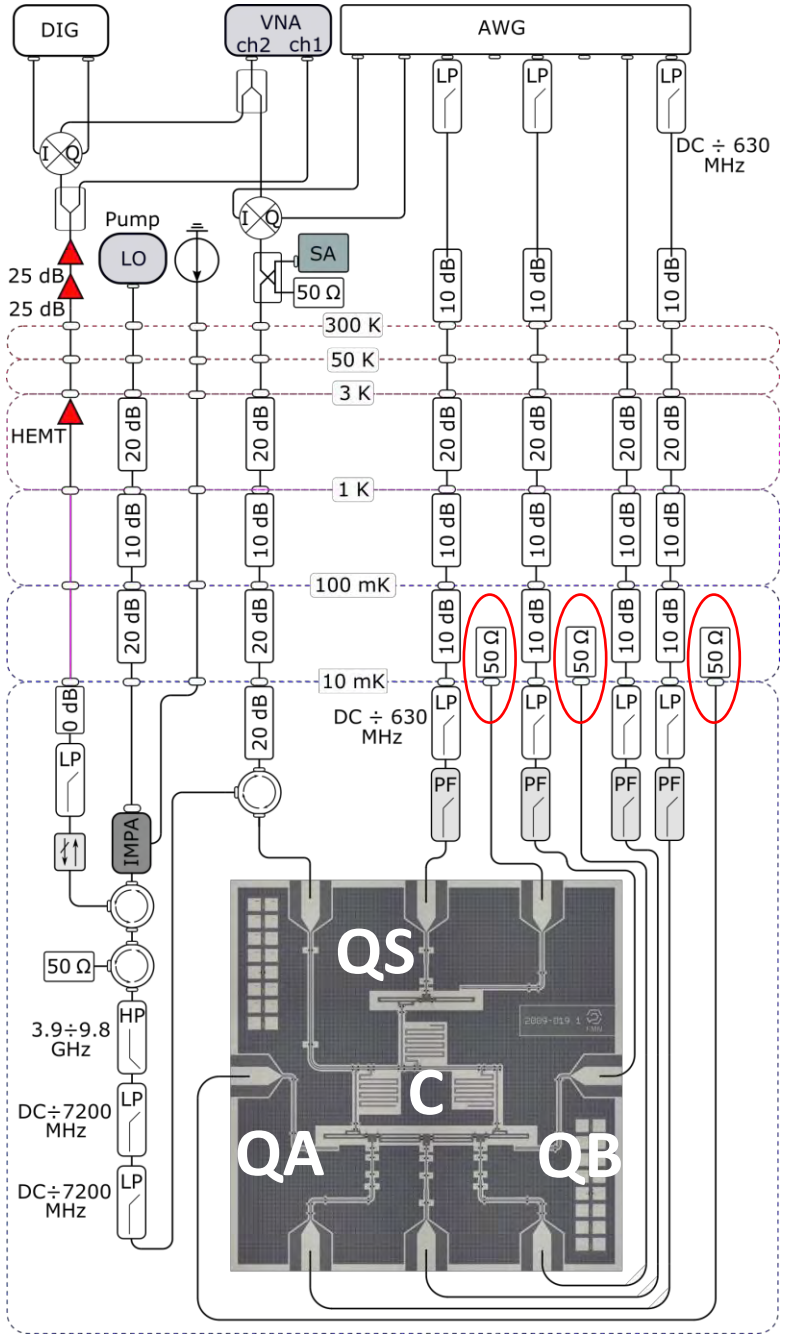
HP — High-Pass Filter (HP)